Accepted Manuscript

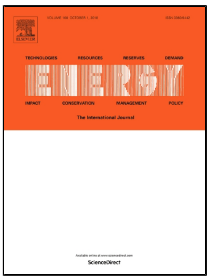

Passive design optimization of low energy buildings in different climates

Fatima Harkouss, Farouk Fardoun, Pascal Henry Biwole

PII:	S0360-5442(18)31779-1
DOI:	10.1016/j.energy.2018.09.019
Reference:	EGY 13713
To appear in:	*Energy*
Received Date:	01 April 2018
Accepted Date:	04 September 2018

Please cite this article as: Fatima Harkouss, Farouk Fardoun, Pascal Henry Biwole, Passive design optimization of low energy buildings in different climates, *Energy* (2018), doi: 10.1016/j.energy.2018.09.019

Passive design optimization of low energy buildings in different climates

Fatima Harkouss [a, b], Farouk Fardoun [a], Pascal Henry Biwole [c, d]

[(a)] University Institute of Technology, Department GIM, Lebanese University, Saida, Lebanon

[(b)] Université Cote d'Azur, J.A. Dieudonné Laboratory, UMR CNRS 7351, Parc Valrose 06108 Nice, France

[(c)] Université Clermont Auvergne, CNRS, SIGMA Clermont, Institut Pascal, F-63000 Clermont–Ferrand, France

[(d)] MINES Paris Tech, PSL Research University, PERSEE - Center for Processes, Renewable Energies and Energy Systems, CS 10207, 06 904 Sophia Antipolis, France

Highlights

-Residential building's passive design parameters are optimized

-Effect of different climates of Köppen Geiger classification is studied

-Thermal comfort and energy performance of the case-studies are significantly enhanced

-Passive cooling strategies lead to adequate thermal comfort and fewer cooling systems

Abstract

Worldwide, the residential buildings are consuming a considerable amount of energy. The high potential of buildings towards energy efficiency has drawn special attention to the passive design parameters. A comprehensive study on optimal passive design for residential buildings is presented in this paper. Twenty-five different climates are simulated with the aim to produce best practices to reduce building energy demands (for cooling and heating) in addition to the life-cycle cost (LCC). The occupants' adaptive thermal comfort is also improved by implementing the appropriate passive cooling strategies such as blinds and natural ventilation. In this respect, the implemented methodology is composed of four phases: building energy simulation, optimization, Multi-criteria Decision Making (MCDM), sensitivity study, and finally an adaptive comfort analysis. An optimal passive solution of the studied building indicates the potential to save up to 54%, 87% and 52% of the cooling demands (Qcool), heating demands (Qheat) and LCC respectively with respect to the initial configuration. The obtained optimal passive parameters are validated with the National Renewable Energy Laboratory NREL benchmark for low energy building's envelope. Additionally, the integrated passive cooling strategies have demonstrated its competency since it leads to a significant overheating decrease.

Keywords: *Building envelope, Passive cooling strategies, Optimization, Decision making, Climate, Life cycle cost, Adaptive thermal comfort*

Nomenclature

AC	Air Conditioner
ACH	Air Changer per Hour
AHP	Analytical Hierarchical Process
ANN	Artificial Neural Network
A_W	Windows area (m^2)
C	Concordance index
CDD	Cooling Degree Days
CI	Consistency Index
D	Discordance index
DM	Decision Maker
EC	Annual Energy Cost ($)
ELECTRE	ELimination and Choice Expressing REality
F1, Fn	Fitness values
GA	Genetic Algorithm
GPS	Generalized Pattern Search algorithm
GPSPSOCCHJ	Generalized Particle Swarm Optimization with Hook Jeeves algorithm
g-value	Solar energy transmittance
HDD	Heating Degree Days
HVAC	Heating, Ventilation, and Air Conditioning
H	Windows height (m)
IC	Initial cost ($)
LCA	Life Cycle Assessment
LCC	Life Cycle Cost
LCIA	Life Cycle Impact Assessment
LPD	Long-term Percentage of Dissatisfied
MCDM	Multi-Criteria Decision Making
MOABC	Multi-Objective Artificial Bee Colony
MOBO	Multi-Objective Building Optimization tool
MOGA	Multi-Objective Genetic Algorithm
MOO	Multi-Objective Optimization
MOPSO	Multi-Objective Particle Swarm Optimization
NREL	National Renewable Energy Laboratory
N	Life period (year)
N	Population size
NED	Net Energy Deficit
NPV	Net Present Value
NSGA-II	Non-Dominated Sorting Genetic Algorithm
PMV	Predicted Mean Votes

PPD	Predicted Percentage of Dissatisfied
PROMETHEE	Preference Ranking Organization METHod for Enrichment of Evaluations
Pt	Parent population
PRMSE	Percentage root mean square error (%)
Qcool	Cooling demand (kWh/y.m^2)
Qheat	Heating demand (kWh/y.m^2)
Qt	Child descendant population
Rt	Initial population
rd	Annual Discount Rate (%)
r	Objective functions number
RMSE	Root mean square error (kWh/y.m^2)
S	Credibility index
SS	Sequential research
TOPSIS	Technique for Order of Preference by Similarity to Ideal Solution
TPES	Total Primary Energy Supply
TSA	Tabu Search Algorithm
T_i	Indoor operative temperature (˚K)
T_{rm}	Exponentially weighted running mean of outdoor dry-bulb air temperature (˚K)
ΔT	Mean temperature difference between inside and outside (˚K)
USPW (N, rd)	Uniform Series Present Worth factor (years)
V	Room volume (m^3)
V_W	Mean wind speed (m/s)
WPM	Weighted Product Method
WSM	Weighted Sum Method
WWR	Window to Wall Ratio

1. Introduction

Buildings (residential, commercial and public) have consumed more than 30% of worlds' total primary energy supply (TPES) since 2014. The residential sector accounts for more than 65% TPES consumption in buildings [1]. Under these circumstances, it is critical to ameliorating the buildings' energy efficiency, since the energy demand is predicted to increase by 50% in 2050 when compared to 2013 [2].

The high potential of buildings towards energy efficiency has drawn special attention to the passive design parameters i.e. building envelope characteristics and passive strategies namely natural ventilation, shading devices, overhangs, and daylighting.

Researchers worldwide are investigating the applicability of building optimization methodologies in order to enhance buildings' energy performance. The investigated methodologies are aimed to facilitate the finding of a unique optimal solution which satisfies both sides: the designer-architecture, and benchmarks regulations. Adopting one optimal passive design recommendation for each climate is a fundamental way to help the buildings to become energy efficient, especially for residential buildings. Even though the optimal passive design solution is related to many factors such as the local climate, building utilization, topography and landscape design.

It is worth mentioning the following definitions used in this study: passive parameters are variables related to building envelope such as the type of walls, roof, ground, windows, window to wall ratio (WWR), and building shape. Passive strategies are scenarios implemented during the building operation such as blinds, overhangs, and natural ventilation with the aim to reduce thermal and lighting demands while ensuring thermal comfort.

An overview of recently investigated optimization problems in the literature [3–46] is represented in Table 1. The summary includes the most examined passive parameters/strategies. The objective functions under investigation are divided into five categories: Economy, energy, environment, comfort, and others. Besides, the adopted optimization algorithms and Multi-criteria Decision Making (MCDM) techniques are stated. Advantages and disadvantages of different optimization algorithms are addressed and summarized in Table 2 [47–51]. Finally, most used sensitivity analysis or uncertainty quantification methods are reviewed. They are used with the aim to test the robustness of the optimal solution on different conditions related to algorithms setting parameters, design/fabrication errors, decision maker (DM) preferences, and energy costs.

Table 1 Overview of the largely optimized passive parameters including the optimization characteristics (Data source: *[3–46]*)

<table>
<tr><th>Investigated parameters</th><th>Objective functions</th></tr>
<tr><td>Thermal transmittance: walls, roof, floor, windows frame, and glazing. Wall thermal, solar, and visible absorptance. Wall emissivity. WWR. Number of windows. G-value of glazing. Glazing solar and visible transmittance. Windows opened area % (Natural ventilation). Overhang tilt angle and depth. Sunshade type. External and internal shading systems. Control strategy of shading devices. Building shape. Relative compactness. Aspect ratio. Ceiling height. Building orientation. House area. Air tightness/ Infiltration rate. Convection coefficients. Vegetation.</td><td rowspan="3">Economy:
Minimize: Life cycle cost (LCC), overall investment cost, lifetime utility cost, building operation cost. Maximize Net present value (NPV).
Energy:
Minimize: Total electricity load, lighting energy consumption. Net energy deficit (NED).
Environment:
Minimize: life cycle environmental impact, Life cycle impact assessment (LCIA), life cycle carbon emissions.
Comfort:
Minimize: Predicted mean votes (PMV), summer thermal discomfort, winter thermal discomfort, visual discomfort, seasonal long-term discomfort indices (=Long-term Percentage of Dissatisfied (LPD) in summer and winter), Predicted Percentage of Dissatisfied (PPD).
Others:
Minimize: shape coefficient. Maximize: window opening rate, thermal admittance, solar radiation gain, space efficiency.</td></tr>
<tr><th>Constraints</th></tr>
<tr><td>NED ≤ 0. Heating loads ≤ 15 kWh/m^2. Annual space energy requirements ≤ 5 Mj/m^2. Air change rate ≥ 0.6 ACH. Area availability. Total window width ≤ Floor width. Windows' area must guarantee adequate natural illumination and ventilation. Acceptable ranges of envelope components' thermal transmittances. Budget constraint. Constraints on design variables. Maximum discomfort hours fixed at 200 h up to 350 h. PMV ≤ 0.5-0.7. Construction budget. Life cycle cost budget.</td></tr>
<tr><th colspan="2">Algorithms</th></tr>
<tr><td colspan="2">Generalized pattern search algorithm (GPS), Multivariate optimization, Particle swarm optimization (PSO), Non-dominated sorting genetic algorithm (NSGA-II), Genetic algorithm (GA), Life Cycle Assessment (LCA), Artificial neural network (ANN), Generalized particle swarm optimization with Hook Jeeves algorithm (GPSPSOCCHJ), Sequential research (SS), Tabu search algorithm (TSA), Artificial bee colony (ABC).</td></tr>
<tr><th colspan="2">MCDM/Sensitivity analysis-Uncertainty quantification</th></tr>
<tr><td><u>Decision making:</u>
Weighted sum method (WSM), Weighted product method (WPM), Decision making: Technique for order of preference by similarity to ideal solution (TOPSIS), Analytical Hierarchical Process (AHP), Elimination and Choice Expressing Reality (ELECTRE) methods, Preference Ranking Organization Method for Enrichment of Evaluations (PROMETHEE) methods.</td><td><u>Sensitivity analysis-Uncertainty quantification:</u>
Impact of: energy prices, discount rates, CO2 emissions prices, climate, utility rates, operating points (heating and cooling set-points). Sensitivity of algorithms parameters. Objective function weights. DM preferences thresholds. Uncertainties in design variables according to probabilistic distributions.</td></tr>
</table>

Table 2 Advantages and disadvantages of optimization algorithms (Data source: [47–51])

Optimization algorithm	Advantages	Disadvantages
PSO	It is based on intelligence. No overlapping and mutation calculation. Research is a very fast and simple computation.	The partial optimism. Which causes the less accuracy at the regulation of PSO speed and the direction. It doesn't work out the problems of scattering and optimization. It doesn't work out the problems of the non-coordinate system (for example solution to the energy field).
LCA	It includes the production or consumption of resources. It provides a complete picture of the problem. It offers a strong environmental tool toward sustainability. It allows the manufacturer to evaluate any change in the production timeline.	It is very specific. It cannot be transposed across to similar operations. Sometimes inventory data is difficult to obtain and best estimates need to be used. Pulling together data can be time-consuming and costly.
GA	It can find fit solutions in a short time. The random mutation guarantees to see a wide range of solutions. Coding is easy compared to other algorithms.	No guarantee to find the most optimal solution. It is hard to choose parameters like a number of generations, population size etc. The choice of other fitness function, genetic encoding, and genotype to phenotype mapping are important in the efficacy of the system. Time is taken for convergence.
TSA	It allows the non-improving solution to be accepted in order to escape from a local optimum. The use of the Tabu list. For large and difficult problems Tabu search can beat other approaches.	Too many parameters to be determined. Very large number of iterations. No guarantee of global optimal solution. Too complex.
ABC	Strong robustness. Fast convergence. High flexibility. Fewer setting parameters.	The early convergence in the later search period. The accuracy of the optimal value cannot meet the requirements sometimes.
NSGA-II	Reliability. Good performance. Effectiveness. Elitism doesn't allow an already found Pareto optimal solution to be deleted.	The crowded comparison can restrict the convergence.

This paper follows the MCDM methodology for buildings energy performance optimization introduced by the authors early [45]. The aim of the chosen method is to identify the best design solution from a set of Pareto-front solutions, a solution which reflects the DM preferences. The implemented simulation-based methodology is composed of four steps: building energy simulation, optimization, MCDM and finally a sensitivity study to test the robustness of the optimal result.

According to the European standard EN 15251: "An energy declaration without a declaration related to the indoor environment makes no sense. Therefore, there is a need for specifying criteria for the indoor environment for design, energy calculations, performance and operation of buildings" [52]. These criteria are related to the occupants' thermal comfort [42,53–61].

The objective of the present paper is to comprehensively investigate the optimal passive design for a case study residential building. Twenty-five different climates from Köppen Geiger classification are simulated with the aim to produce best practices to minimize building energy demands (cooling and heating) in addition to the LCC. The occupants' adaptive thermal comfort is also inspected aiming at getting more practical and detailed passive design solutions.

So, an additional step is added to the adopted methodology, which is the introduction of adequate passive cooling strategies (natural ventilation, shading devices) that ensure to the maximum extent the occupant's adaptive comfort in the optimal model.

At first, the base case design conditions including building model, operating points, different representative cities for each climate and the corresponding simulation results are described. Then, a wide range of passive design measures is optimized for each climate, including wall and roof insulation levels, windows glazing type, WWR at each facade. Besides, in order to obtain a robust unique solution, a MCDM technique and sensitivity analysis are employed. Then, the impact of implementing shading devices and natural ventilation on the optimal building's energy consumption in different climates is investigated by comparing the overheating hours' percentage. Finally, a set of general recommendations is outlined in order to improve the energy and comfort performances of residential buildings depending on the climate.

2. Base case building and investigated climates

2.1. Building model and design conditions

The base case model is a generic residential building composed of three typical floors. Each floor is 205 m^2 divided into two apartments noted A and B, as shown in Figure 1. Building's net area (excluding balconies, bathrooms, lobbies and non-conditioned spaces) is 432.6 m^2.

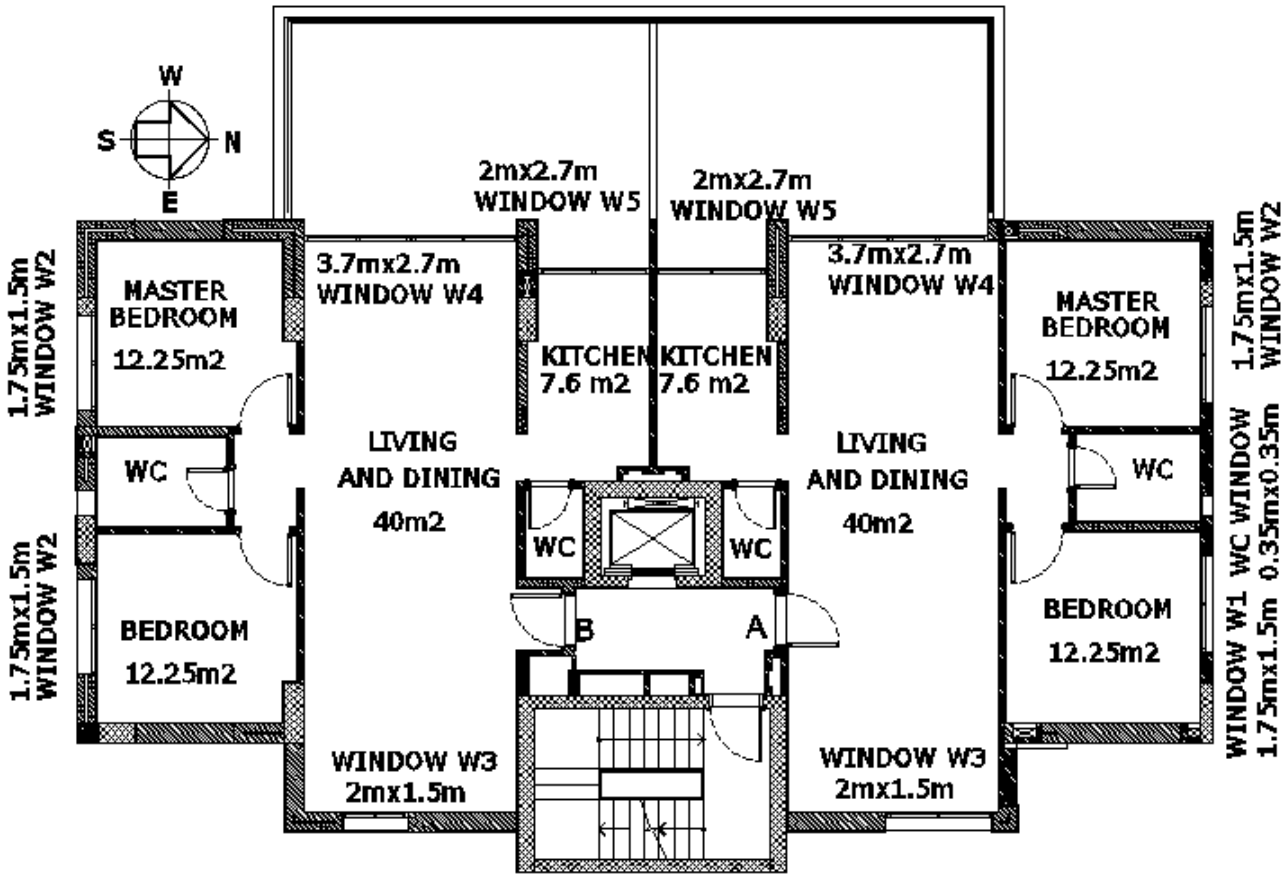

Figure 1 Typical floor plan of the base case building

The thermo-physical characteristics of the building's envelope are represented in Table 3. This research work is based on the assumption that the thermophysical properties are considered to be constant. Even though some studies in the literature have addressed building optimization with variable thermo-physical properties [62–65].

WWR at Northern, Southern, Eastern and Western façades are 22%, 22%, 25% and 84% respectively. Windows use insulating double glazing with Argon 4/16/4, having a thermal transmittance of 1.4 $W/m^2.K$ and a g-value of 0.6, without shading devices, overhangs nor blinds.

Table 3 Thermo-physical characteristics of building's envelope (Properties: data source [66])

Building envelope Overall thermal transmittance	Components (From inside to outside)	Thickness (cm)	Thermal Conductivity (W/m.K)	Density (kg/m³)	Specific Heat (J/kg·K)
External Wall 0.46 W/m2.K	Plaster	2	0.72	1860	840
	Concrete masonry unit	10	1.3	2240	800
	Extruded Polystyrene	5	0.029	29	1210
	Concrete masonry unit	15	1.3	2240	800
	Plaster	2	0.72	1860	840
Internal Wall 3.30 W/m².K	Plaster	2	0.72	1860	840
	Concrete masonry unit	10	1.3	2240	800
	Plaster	2	0.72	1860	840
Internal Floor 2.65 W/m².K	Marble	0.8	3.5	2800	1000
	Lime mortar	0.3	0.87	1800	1000
	Sand gravel	0.5	0.7	1800	1000
	Reinforced concrete	30	1.8	2500	840
	Plaster	2	0.72	1860	840
Ground 2.60 W/m².K	Marble	0.8	3.5	2800	1000
	Lime mortar	0.3	0.87	1800	1000
	Sand gravel	0.5	0.7	1800	1000
	Waterproofing	-	-	-	-
	Extruded Polystyrene	0	0.029	29	1210
	Reinforced concrete	30	1.8	2500	840
Roof 1.58 W/m².K	Plaster	2	0.72	1860	840
	Reinforced concrete	15	1.8	2500	840
	Extruded Polystyrene	1	0.029	29	1210
	Waterproofing	-	-	-	-
	Asphalt roll	0.5	0.75	1100	1510

Each apartment is housing a family of four persons, the adopted occupants' schedule of presence in the living and dining room, kitchen and bedrooms is represented in Figure 2.

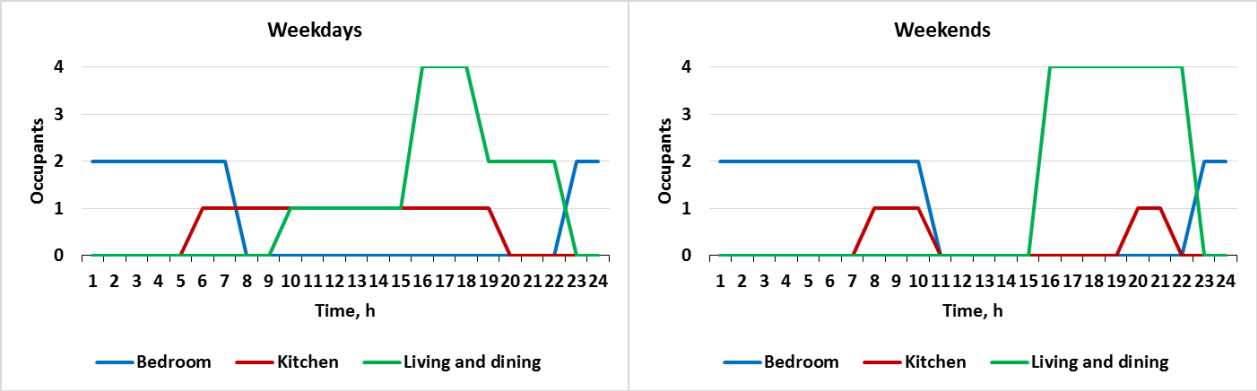

Figure 2 Occupants' schedule of presence in living and dining, kitchen and bedrooms

The infiltration rate for a single-family home at low leakage level is 0.4 ACH at Q4Pa (4.5 $m^3/h.m^2$ of floor area at Q50Pa) according to EN 15242 [67]. The adopted unoccupied hour ventilation rate in this model is 0.075 $L/s.m^2$. During occupied hours the minimum specified ventilation air change rate, for new residential buildings with a normal level of expectation, is 0.42 $L/s.m^2$ assuming continuous operation and complete mixing of air [52].

The lighting illuminance level for residential buildings is chosen based on recommendations of EN 12464-1 [68]. An illuminance level of 100 lux is chosen for bedrooms and 200 lux for kitchens and dining rooms. Fluorescent lighting fixtures with a luminous efficiency of 60 lm/W are implemented corresponding to occupants' schedule of presence. The adopted electric appliances in each apartment include a computer, TV in living rooms, washing machine, refrigerator, electric oven, extraction hood in kitchens, and toilet exhaust fans. The hourly appliances electrical consumption is given in Figure 3 [66,69].

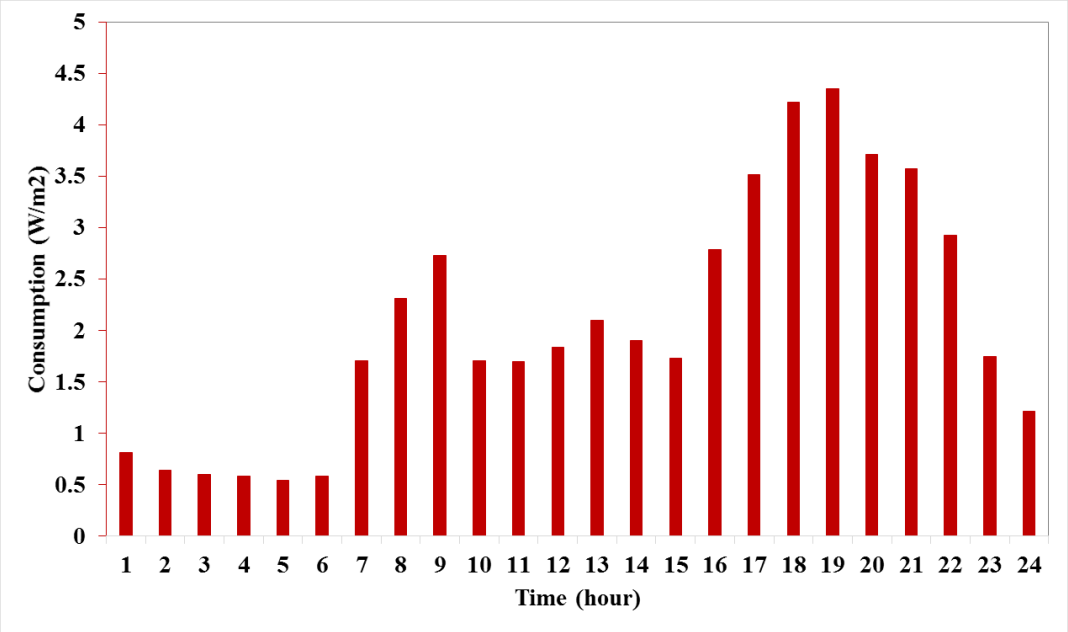

Figure 3 Hourly appliances consumption (W/m^2) (Data source: *[66,69]*)

Based on the type of building, a consistent interval for indoor operative temperature (T_i) is recommended by EN 15251 [52] in order to appropriately dimension cooling and heating systems. For recent residential building, the recommended T_i in living space under the metabolic rate of 1.2 met are as follows: T_i (˚C) = 20-25 ˚C for heating (Clothing ~ 1 clo) and T_i (˚C) = 23-26 ˚C for cooling (Clothing ~ 0.5 clo). The settings for sizing cooling and heating systems are respectively the upper and lower values of the comfort range, i.e. 26 ˚C and 20 ˚C according to occupants' schedule of presence. In this study an air source-heat pump of COP = 2.9 and gas boiler of 98.3% efficiency are used as cooling and heating systems. Commonly, humidification or dehumidification is desired only in distinctive buildings like industries, health care facilities, museums etc. [52]. So, humidification and dehumidification are turned off in this model.

2.2. Building model validation

The simulated building model on TRNSYS is validated with the National Institute of Standards and Technology (NIST) residential test facility in Gaithersburg, USA [70]. The NIST test facility design conditions, summarized in Table 4, are integrated into the TRNSYS model to simulate the cooling and heating loads. Table 5 and Figure 4 represent the comparison between measured and simulated cooling and heating loads. The agreement between experimental data and simulated results is estimated using the root mean square error (RMSE) and the percentage root mean square error (PRMSE). The measured loads are slightly different than the simulated ones which indicate that TRNSYS building simulations and NSIT experimental measures are in good agreement.

Table 4 NSIT test facility design conditions (Data source *[70,71]*)

Design conditions	**Value**
External walls thermal transmittance, W/m^2.K	0.13
Roof thermal transmittance, W/m^2.K	0.08
Ground floor thermal transmittance, W/m^2.K	0.56
Windows thermal transmittance, W/m^2.K	1.14
WWR at Northern façade, %	16.4
WWR at Southern façade, %	23.2
WWR at Eastern façade, %	7.4
WWR at Western façade, %	5
Cooling set point, ˚C	23.8
Heating set point, ˚C	21.1
Cooling mode dehumidification relative humidity, %	50

Table 5 Measured and simulated thermal loads (Data source *[70,71]*)

	NIST measures kWh/y.m^2	**TRNSYS simulation kWh/y.m^2**	**RMSE kWh/y.m2**	**PRMSE**
Cooling load,	27.73	26.16	1.56	4%
Heating load,	30.57	29.31	1.26	6%

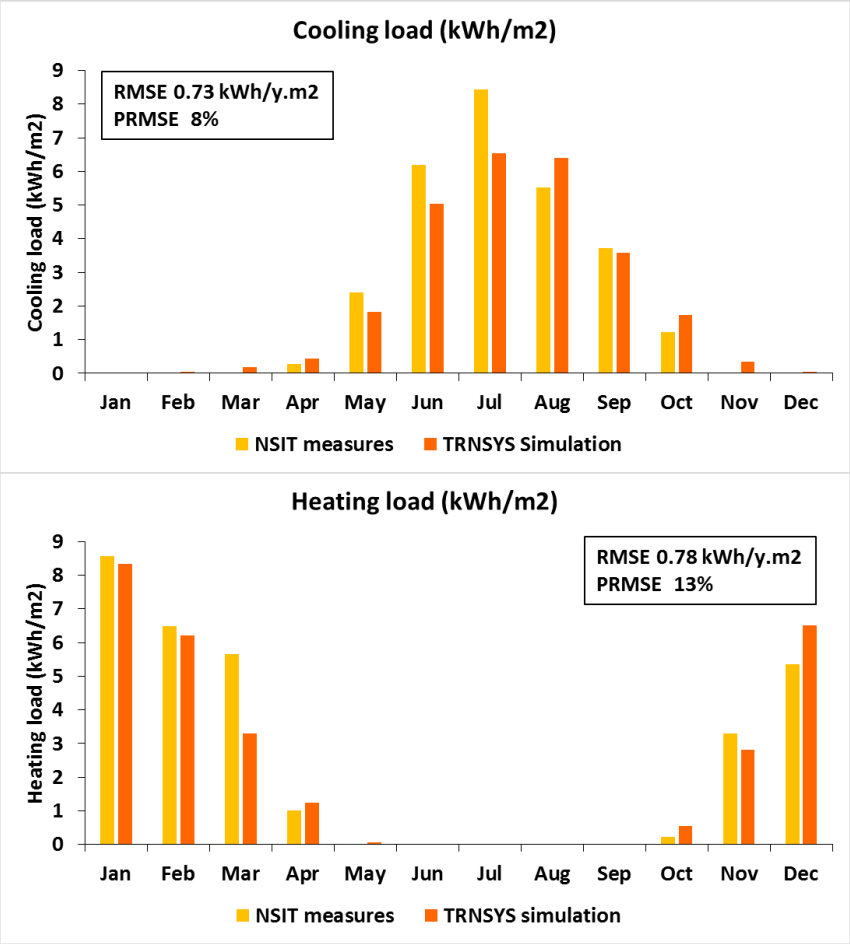

Figure 4 Monthly measured and simulated thermal loads (Data source *[70,71]*)

2.3. Investigated climates

In this work, the Köppen-Geiger climates classification is adopted [72]; Figure 5. This classification divides the world into five main climatic zones based on the average annual precipitation, the average monthly precipitation, and the mean monthly temperature. The zones are A: equatorial, B: arid, C: warm temperate, D: snow, and E: polar. The level of precipitation is defined as W: desert, S: steppe, f: fully humid, s: summer dry, w: winter dry, and m: monsoonal. Besides, the temperature is provided as h: hot arid, k: cold arid, a: hot summer, b: warm summer, c: cool summer, d: extremely continental, and F: polar frost. In the current study, one city of each dominant climatic zone is selected. Table 6 presents the twenty-five selected cities' geographical information in addition to cooling degree days (CDD) and heating degree days (HDD). The CDD 10˚C and HDD 18˚C are computed using TRNSYS software. The degree days are the sum (on a yearly basis) of the temperature difference between the average daily outdoor temperature and a

base temperature which is the indoor temperature that a cooling/heating system should compensate to satisfy the comfort requirements.

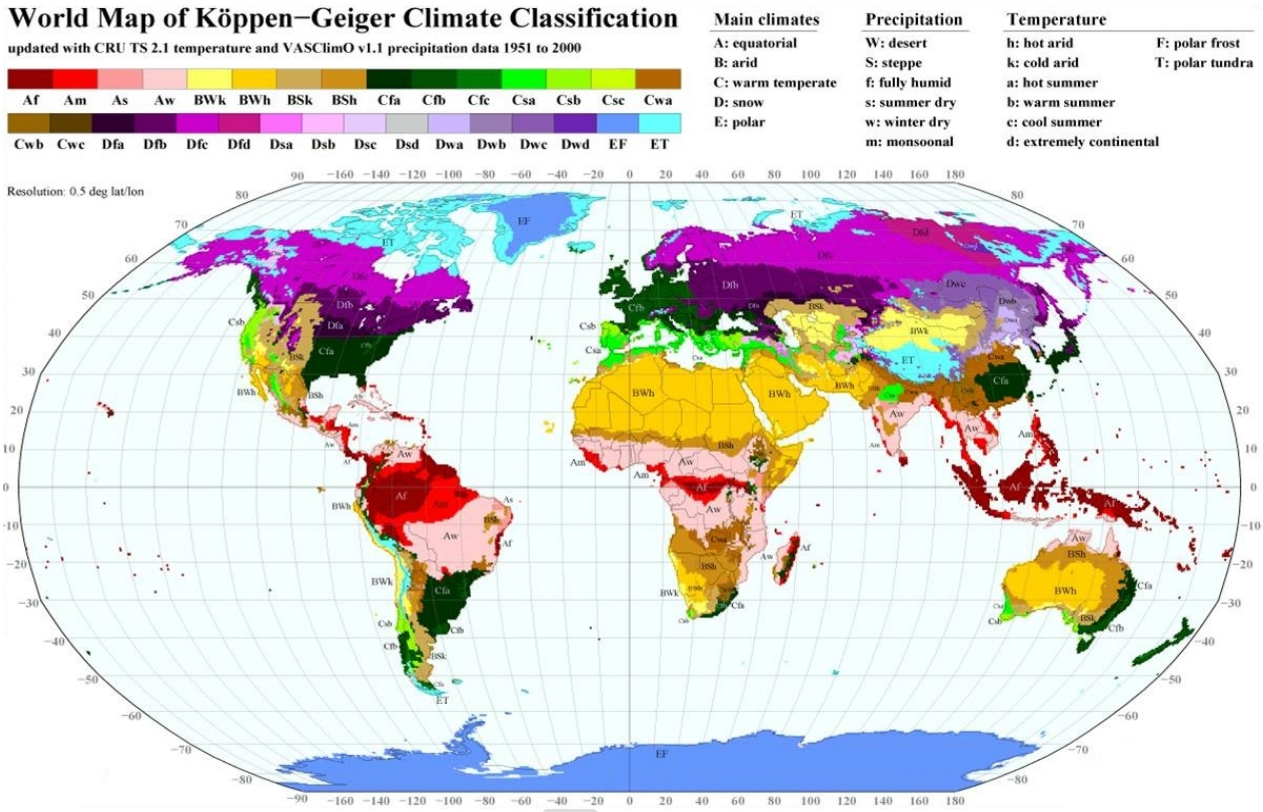

Figure 5 World Map of Köppen–Geiger climate classification *[72]*

Table 6 Selected cities and climate characteristics (Data source: *[72,73]*)

Climatic Zone	City	Altitude (m)	Longitude, Latitude	CDD base 10˚C	HDD base 18˚C
Af	Singapore	16	104.00˚E, 1.03˚N	6058	0
Am	Douala (Cameroon)	5	9.70˚E, 4.00˚N	6037	0
As	Indore (India)	567	75.80˚E, 22.70˚N	5400	54
Aw	Caracas (Venezuela)	43	66.98˚W, 10.60˚N	5819	0
BSh	Dakar (Senegal)	20	17.47˚W, 14.73˚N	5242	0
BSk	Baku (Azerbaijan)	5	49.85˚E, 40.38˚N	2262	2091
BWh	Abu Dhabi (UAE)	27	54.65˚E, 24.43˚N	6068	28
BWk	Esfahan (Iran)	1590	51.67˚E, 32.62˚N	2826	1895
Cfa	Milan (Italy)	103	9.28˚E, 45.43˚N	1528	2651
Cfb	Nancy (France)	212	6.20° E, 48.70° N	907	3228
Csa	Sacramento (USA)	8	121.5° W, 38.5° N	2349	1467
Csb	Ankara (Turkey)	902	32.88˚E, 39.95˚N	1607	2735
Csc	Cedars (Lebanon)	1832	36.03°E, 34.25°N	1539	2605
Cwa	New Delhi (India)	212	77.20°E, 28.58°N	5454	230
Cwb	Kunming (China)	16	102.70°E, 25.00°N	1814	202
Dfa	Sapporo (Japan)	17	141.33°E, 43.05°N	1183	3808
Dfb	Montreal (Canada)	133	73.62°W, 45.50°N	1126	4507
Dfc	Tromso (Norway)	102	18.95°E, 69.65°N	120	5525
Dfd	Kotelny Island (Russia)	11	137.90°E, 76.00°N	0	12073
Dsa	Hakkari (Turkey)	1720	43.77°E, 37.57°N	1663	3425
Dsb	Dras (India)	3100	75.76°E, 34.43°N	620	5921
Dwa	Beijing (China)	55	116.28°E, 39.93°N	2125	3046
Dwb	Khabarovsk (Russia)	87	135.17°E, 8.52°N	1021	6126
Dwc	Chita (Russia)	671	113.33°E, 52.02°N	576	7593
ET	Barentsburg (Norway)	75	14.22°E, 78.07°N	0	8517

3. Simulation of the base case model

The building annual energy consumptions, costs, and comfort are simulated using TRNSYS software, according to the above-mentioned design conditions. In order to evaluate the building model cost-effectiveness, LCC is adopted. LCC is the most frequent method to estimate the financial benefits of energy conservation projects over their lifetime [18,74]. The LCC is given by:

$$\mathrm{LCC}\ (\$) = \mathrm{IC} + \mathrm{USPW}\ (\mathrm{N}, \mathrm{rd}) \times \mathrm{EC} \qquad \text{eq. 1}$$

$$\mathrm{USPW}\ (\mathrm{N}, \mathrm{rd}) = \frac{1 - (1 + \mathrm{rd})^{-\mathrm{N}}}{\mathrm{rd}} \qquad \text{eq. 2}$$

where, IC stands for the initial cost of implementing design and operating conditions for building envelope in addition to heating, ventilation and air conditioning (HVAC) system ($), USPW (N, rd) is the uniform series present worth factor (it converts future recurrent expenses to present costs) (years), Rd is the annual discount rate (%), N stands for the life period (year), and EC is the annual energy cost essential to maintain building's indoor comfort for the selected design and operating conditions ($).

Herein, the life period and discount rate are set to 30 years and 5% respectively [16]. The implementation costs of different design options are represented in Table 7. Figure 6 represents the average energy costs of electricity and gas in each of the investigated cities. It is worth mentioning that the implementation costs of various materials are just indicative due to the potential change in prices in the market.

Table 7 Implementation costs of base case design options (Data source:*[18,75,76]*)

Specification	Options	Cost
Wall insulation, Roof insulation, Ground insulation	Extruded polystyrene	2.6 $/m^2/cm
Glazing type for windows (Thermal transmittance W/m^2.K, g-value)	Double glazing with Argon, 4/16/4 (1.4, 0.58)	110 $/m^2
Air conditioning	-	221.78 $/kW
Boiler	Condensing gas boiler (Efficiency=98.3%)	1900 $/Unit

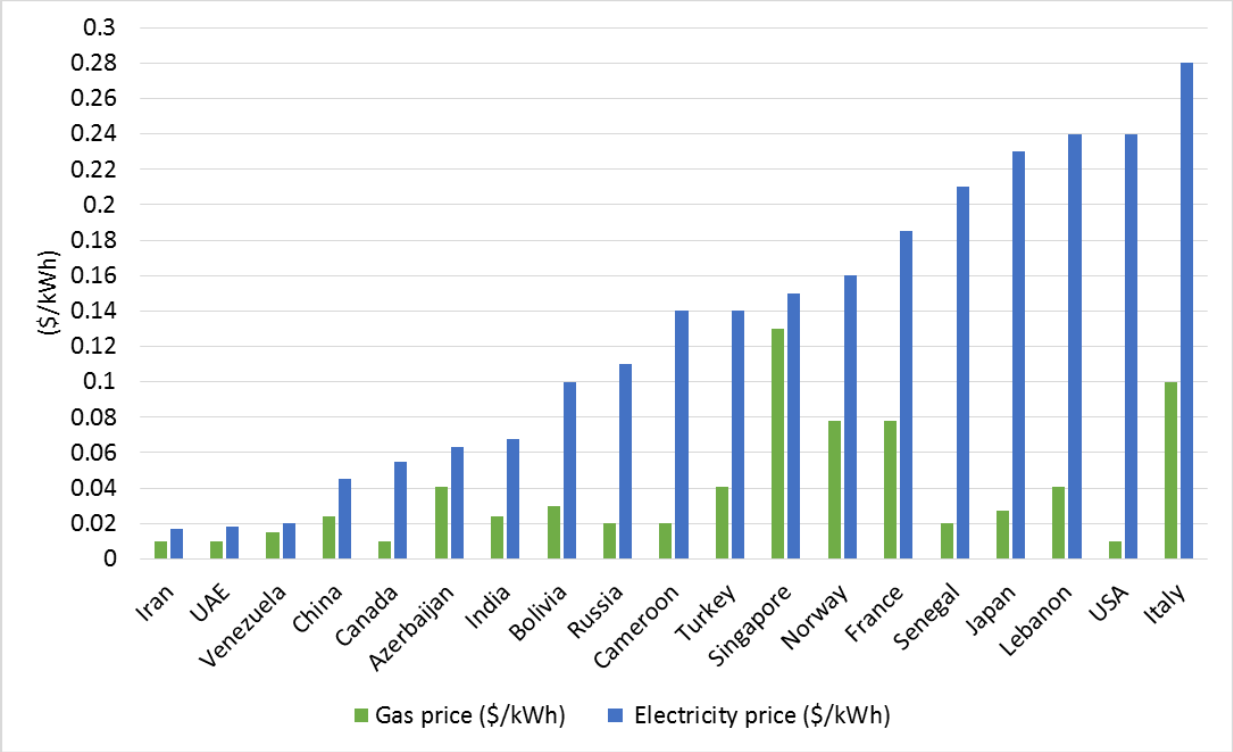

Figure 6 Average energy costs (electricity and gas) in each of the investigated cities (Data source: *[77–90]*)

The simulation phase steps through the TRNSYS simulation tool are represented in Figure 7.

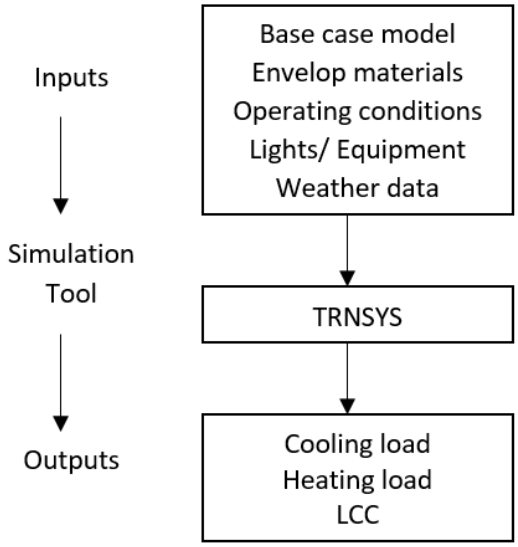

Figure 7 Simulation phase steps to evaluate thermal loads and LCC

Figure 8 represents the annual cooling loads (Qcool), heating loads (Qheat) and 30-years LCC of the base case building in each of the investigated climates.

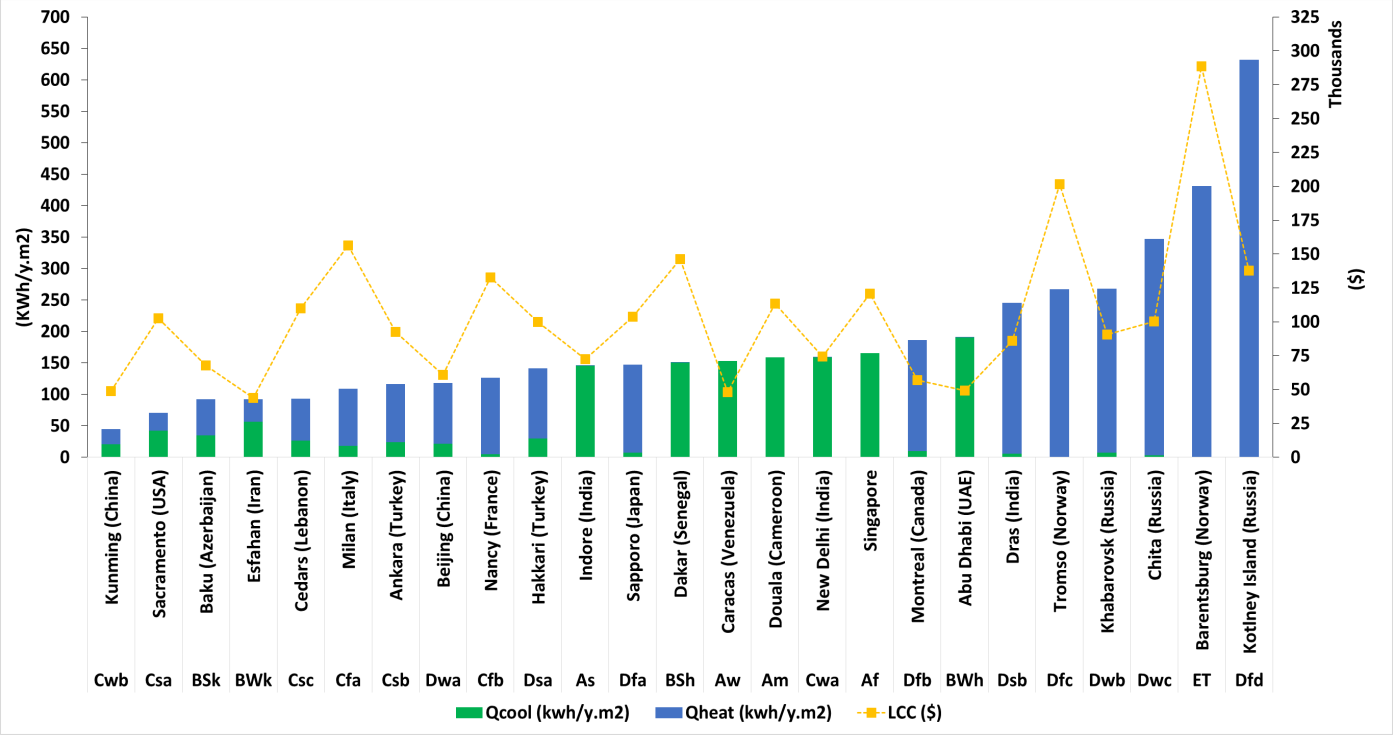

Figure 8 Evaluated Qcool (kWh/y.m^2), Qheat (kWh/y.m^2) and 30-years LCC ($) for each of the investigated climates

Generally from Figure 8 and Table 6, it can be noticed that the cooling load ranges from less than 10 kWh/y.m^2 in climates where the CDD 10˚C < 1200: Tromso, Baretsburg, Kotelny Island, Khabarovsk, Chita., Dras, Nancy, Sapporo, and Montreal, to more than 100 kW/y.m^2 in climates where CDD 10˚C > 3500: Indore, Dakar, Caracas, Douala, New Delhi, Singapore and Abu Dhabi. Conversely, the heating loads variates from less than 10 kWh/y.m^2 in climates where HDD 18˚C < 250: Indore, Dakar, Caracas, Douala, New Delhi, Singapore and Abu Dhabi, to more than 100 kWh/y.m^2 in climates where HDD 18˚C > 3250: Hakkarti, Nancy, Sapporo, Montreal, Dras, Tromso, Baretsburg, Kotelny Island, Khabarovsk, and Chita.

It is clear from Figure 6 and Figure 8 that the LCC mainly depends on two conditions: thermal loads and energy prices in each region. The LCC ranges from less than 50000 $ in Kunming (low thermal loads and energy prices), Esfahan (low thermal loads and energy prices), Caracas (low energy prices) and Abu Dhabi (low energy prices), up to triple, to more than 150000 $ in Milan (high energy prices), Tromso and Barentsburg in Norway (high thermal loads and relatively high gas prices). Even though the thermal load in Milan is the half when compared to other cities such

as Dras, Khabarovsk, Chita and Kotelny Island, the LCC is so much higher due to the high gas cost in Italy (0.1 $/kWh).

Hence, the importance of building multi-objective optimization (MOO) is in taking into account all factors including energy prices and envelope construction materials prices, to ameliorate the base case building energy, economic and comfort performances in each of the investigated climates.

From the above, the three categories of cities might be derived as shown in Table 8. The categories rely on the dominating presence of cooling and/or heating loads in each climate. Category 1 is dominated by heating loads with cooling loads less than 10 kWh/y.m^2. Conversely, category 2 is dominated by cooling loads with heating loads less than 10 kWh/y.m^2. Furthermore, category 3 corresponds to mixed climates where both cooling and heating loads coexist. Each category will be examined separately in order to simplify the finding of one optimal solution related to the dominant load. Noting that when comparing the above categorization with ASHRAE climates classification [91], categories 1, 2 and 3 refer to ASHRAE thermal zones 6 to 8, 0 to 2 and 3 to 5 respectively.

Table 8 Categorization of investigated climatic zones

Category 1 **Heating dominant**	**Category 2** **Cooling dominant**	**Category 3** **Mixed climate**
Nancy (Cfb)	Indore (As)	Baku (BSk)
Sapporo (Dfa)	Caracas (Aw)	Esfahan (BWk)
Montreal (Dfb)	Douala (Am)	Milan (Cfa)
Tromso (Dfc)	Singapore (Af)	Sacramento (Csa)
Kotlney Island (Dfd)	Dakar (BSh)	Ankara (Csb)
Khabarovsk (Dwb)	Abu Dhabi (BWh)	Cedars (Csc)
Chita (Dwc)	New Delhi (Cwa)	Hakkari (Dsa)
Dras (Dsb)		Beijing (Dwa)
Barentsburg (ET)		Kunming (Cwb)

4. Optimization phase

In this study, the optimization is carried out using TRNSYS coupled with MOBO, a Multi-Objective Building Optimization tool developed by Palonen et al. [92]. On the building optimization judgment, MOBO shows promising competences and might become the main optimization engine in coming years, as mentioned by Nguyen et al. [93]. The building simulation and optimization phase steps are summarized in Figure 9.

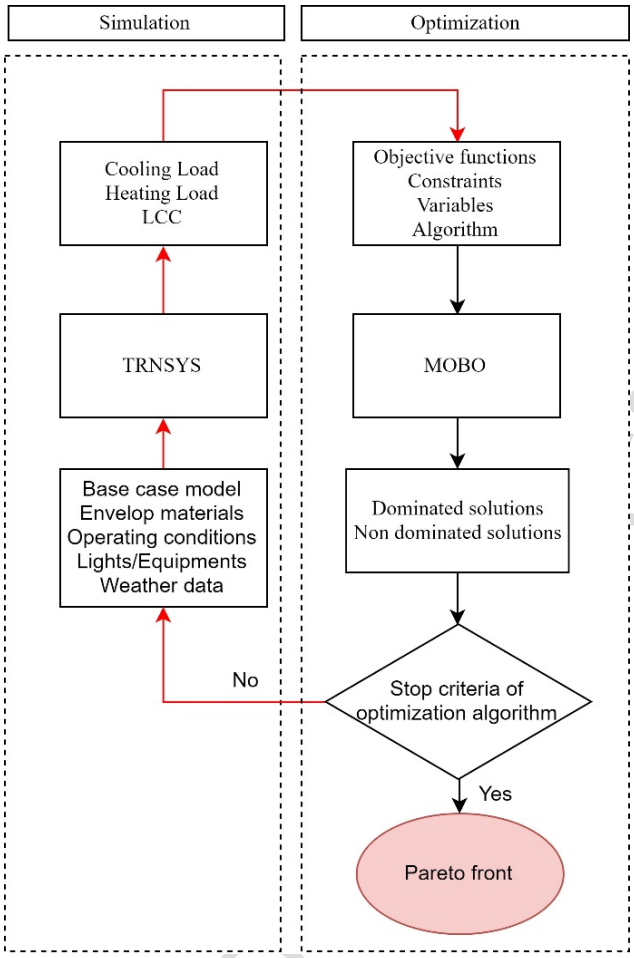

Figure 9 Building simulation and optimization phase steps

4.1. Objective functions

The adopted objective functions in this optimization problem are to minimize building heating load, cooling load, and LCC. Hence, the optimization problem can be summarized as follows:

$$\begin{Bmatrix} \text{Min (Qheat)} \\ \text{Min (Qcool)} \\ \text{Min (LCC)} \end{Bmatrix} \quad \text{eq. 3}$$

4.2. Decision variables

The purpose of this research work is to obtain the optimal passive design solution for the considered residential building model in different climates. From the literature review [3–43], the most suitable design variables to investigate in this work, including their different values, are shown in Table 9. Furthermore, the implementation costs of the different investigated materials are represented in Table 7 and Table 10.

Table 9 Description and different options of decision variables used in the optimization problem

Variable	Value 1	Value 2	Value 3	Value 4	Value 5
External walls thermal transmittance (W/m2.K)	0.2	0.3	0.4	0.5	0.6
Roof thermal transmittance (W/m2.K)	0.2	0.3	0.4	0.5	0.6
Ground thermal transmittance (W/m2.K)	0.2	0.3	0.4	0.5	0.6
WWR at each façade: N, S, E and W (%)	10	30	50	70	90
Glazing Type at each façade: N, S, E and W (Thermal transmittance W/m².K,g-value)	Double glazing with Krypton (0.86, 0.59)	Double glazing with Argon, low-e (1.26, 0.39)	Double glazing with Argon (1.4, 0.58)	Double glazing (2.83, 0.75)	Single glazing (5.68,0.85)

Table 10 Implementation costs of different glazing options used for the optimization analysis (Data source:*[18,75,76]*)

Specification	Options	Cost
Glazing type for windows (Thermal transmittance W/m².K,g-value)	Double glazing with Krypton, 4/16/4 (0.86, 0.59)	145 $/m²
	Double glazing with Argon, low-e 6/16/6 (1.26, 0.39)	120 $/m²
	Double glazing with Argon, 4/16/4 (1.4, 0.58)	110 $/m²
	Double glazing, 4/16/4 (2.83, 0.75)	66 $/m²
	Single glazing (5.68,0.85)	45 $/m²

4.3. Optimization algorithm

The NSGA-II, developed by Deb et al. [47], is a MOO algorithm that can be used in building's optimization [94]. The NSGA-II performs greater than the NSGA in terms of distance to the true Pareto front, size of hyper-volume and spread of optimal points [95,96]. Further overview on the application of NSGA II, could be found in the literature [9,12,22,32,47,97–105]. NSGA-II main process includes population generation, fitness evaluation, and ranking according to crowding distance (estimation of how near an individual is to its neighbors, a large crowding distance reveals a high degree of diversity), elitist selection, bimodal crossover, and mutation [12,22].

The input setting parameters of the NSGA-II adopted in this work is listed in Table 11. These parameters are selected based on the preliminary researches to get the best compromise between the Pareto-front accuracy and the optimization computational time [22].

Table 11 Input setting parameters of NSGA-II

Parameter	Value
Population size	40
Generation number	25
Crossover probability, %	70
Mutation probability, %	2

4.4. Optimization results

In MOO, there is not a practical solution that minimizes/maximizes all objective functions simultaneously. Consequently, more emphasis is paid to Pareto optimal solutions which are not dominated by any other solutions and cannot be upgraded with respect to any objective without worsening at least one objective. In the present work, the three-objective optimization generates a three-dimensional (3D) problem space. Figure 10 represents the Pareto front of Sacramento. In order to simplify the analysis, the 3D-Pareto-front is projected on a bi-dimensional 2D-graph.

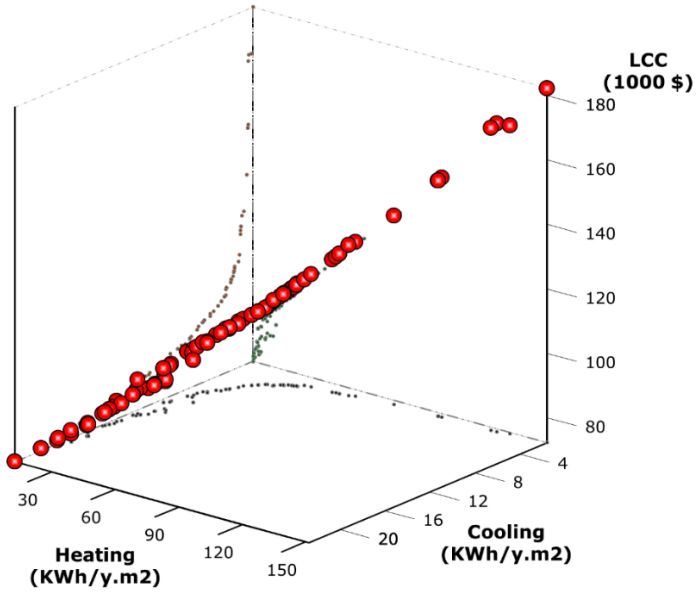

Figure 10 Pareto front of Sacramento in (Qheat, Qcool, LCC) 3D space

The Figures from 11 to 15 illustrate the projection of Pareto fronts in Qcool, Qheat, and LCC plans. Generally, it could be noticed that the scattering of each of the projections for each category is almost parallel in all cities. Even though some scatters are shifted with respect to each other due to particular climates specifications and energy prices.

Figure 11 and Figure 12 illustrate the projection of categories 1 and 2 Pareto fronts in *Qheat, LCC,* and *Qcool*, *LCC* spaces. It is clear that the dispersion of Pareto points is similar in some regions and is different in other ones. For example, the Pareto front in Barentsburg is reduced to very close points, which means that there is a unique solution which minimizes both objectives, Qheat and LCC, at the same time. The same case is found in Caracas, Douala, and Singapore.

The conflict between the three objective functions for all cities of category 3, where both heating and cooling loads exist, is projected on Qcool, Qheat, and LCC plans; Figure 13, Figure 14, and Figure 15. It is obvious from Figure 13 that cooling and heating loads are mostly inversely proportional, except in Beijing and Esfahan where the dispersion of Pareto front points seems to be random. The randomness distribution form of the Pareto front in some scatters is due to the projection in the 2D-space. Some points may appear to be dominated while in fact, they are not. Furthermore, it is noticed that the cooling load and the LCC are almost directly proportional as revealed in Figure 14. Contrariwise, the heating load and the LCC are inversely proportional as shown in Figure 15. This is because electricity is more expensive than gas in all cities and because of the inverse relationship between cooling and heating loads.

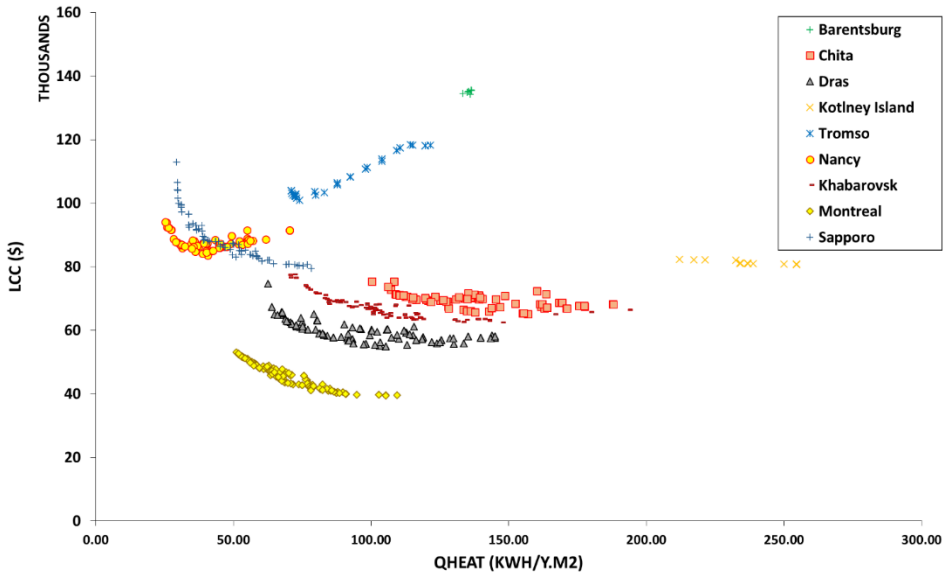

Figure 11 Projection of "Category 1" Pareto front in (Qheat, LCC) 2D-space

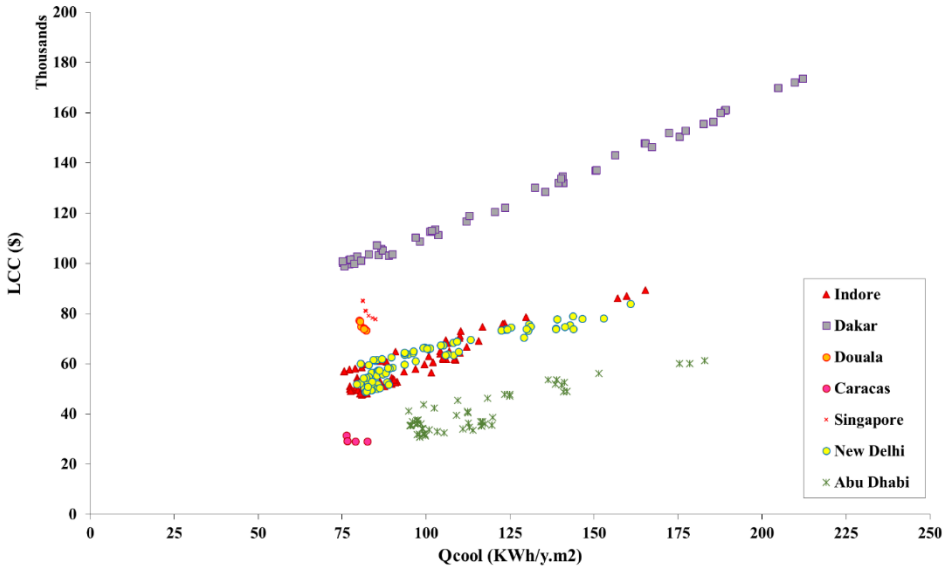

Figure 12 Projection of "Category 2" Pareto front in (Qcool, LCC) 2D-space

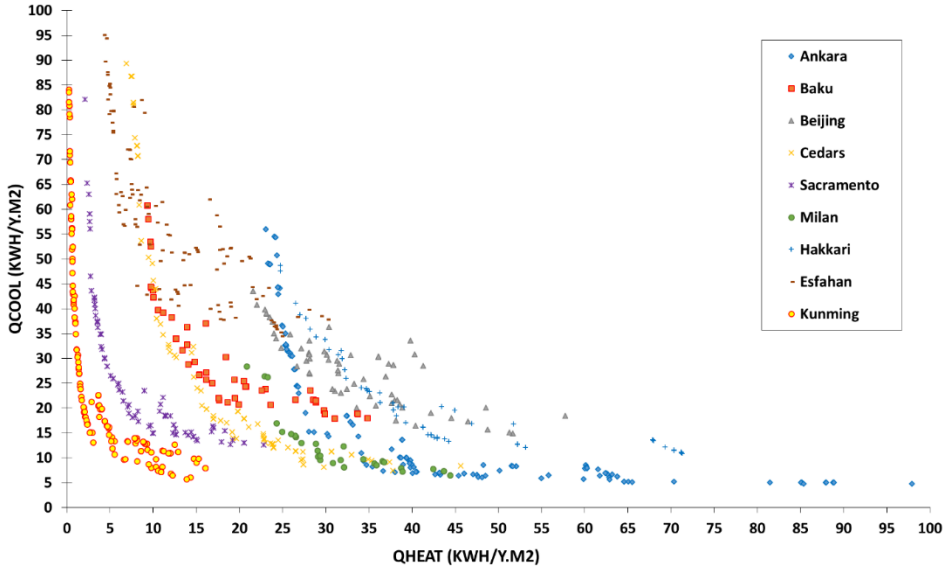

Figure 13 Projection of "Category 3" Pareto front in (Qheat, Qcool) 2D-space

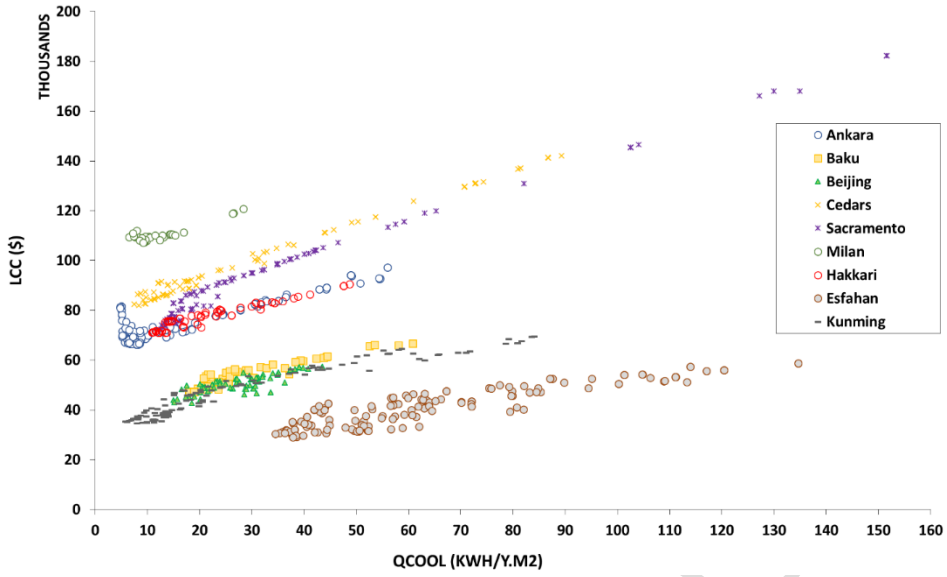

Figure 14 Projection of "Category 3" Pareto front in (Qcool, LCC) 2D-space

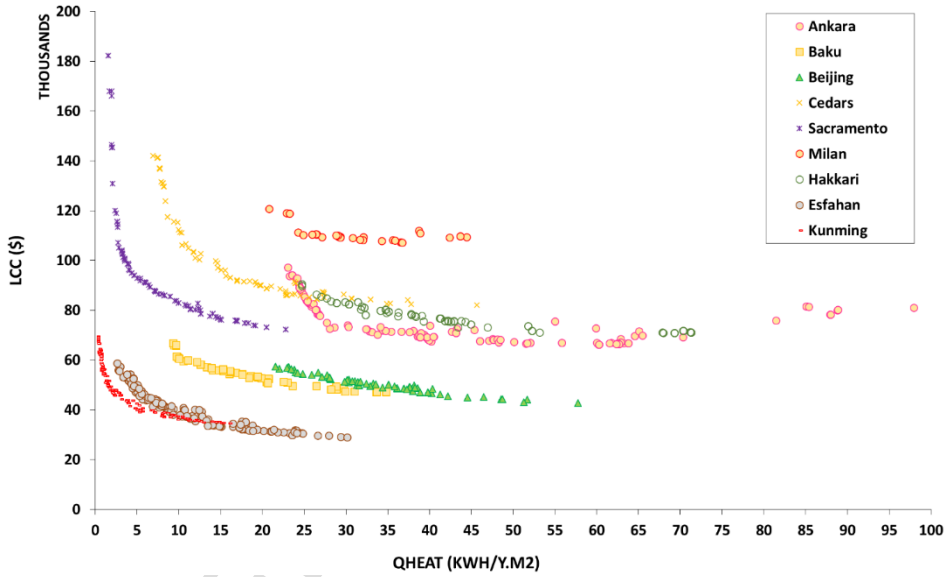

Figure 15 Projection of "Category 3" Pareto front in (Qheat, LCC) 2D-space

5. Optimal solution selection using multi-criteria decision making (MCDM)

Although the Pareto front is found, the ultimate solution of the MOO problem involves the explicit integration of the DM preferences over the different objective functions. In this work, it is decided to use ELECTRE III outranking method [106,107]. The extensive employment of this method in the literature [107–118] against other MCDM techniques, made it the best option to implement in the MCDM phase. Starting with the sets of Pareto front obtained for each category, results of the MOO problem, indifference, preference and veto thresholds of each set are calculated

accordingly as 5%, 10%, and 30% with respect to the average of each objective function. On the other hand, the objective functions weights are calculated by means of the AHP method developed by Saaty [109,119].

5.1. Sensitivity analysis

Since the final result might be heavily influenced by the weights assigned to each objective function, it is useful to perform a sensitivity analysis to identify how the final optimal solution would have changed if the weights would have been different. This is a key phase of the process and, generally, no eventual decision should be taken without performing sensitivity analysis. So as to evaluate the robustness of the optimized solution ranking from the DM point of view, seven different cases are chosen. Table 12 represents the relative weights for each case of objective functions' importance level.

Table 12 Relative weight of each objective function for different DM preferences

Cases	Importance level	Weights		
		Qheat	Qcool	LCC
Case 1	Qheat~Qcool~LCC	0.33	0.33	0.33
Case 2	Qheat > (Qcool, LCC) Qcool~LCC	0.60	0.20	0.20
Case 3	Qcool > (Qheat, LCC) Qheat~LCC	0.20	0.60	0.20
Case 4	LCC > (Qheat, Qcool) Qheat~Qcool	0.20	0.20	0.60
Case 5	Qheat~Qcool (Qheat, Qcool)> LCC	0.43	0.43	0.14
Case 6	Qheat~LCC (Qheat, LCC)> Qcool	0.43	0.14	0.43
Case 7	Qcool~LCC (Qcool, LCC)> Qheat	0.14	0.43	0.43

After applying ELECTRE III on each of the found Pareto fronts for different cities and for different cases of objective functions' weights, the frequent best-ranked solutions are derived. Figure 16 represents the case of Singapore-category 2. S6, S7, and S8 in the figure correspond to the 6^{th}, 7^{th} and 8^{th} Pareto front points.

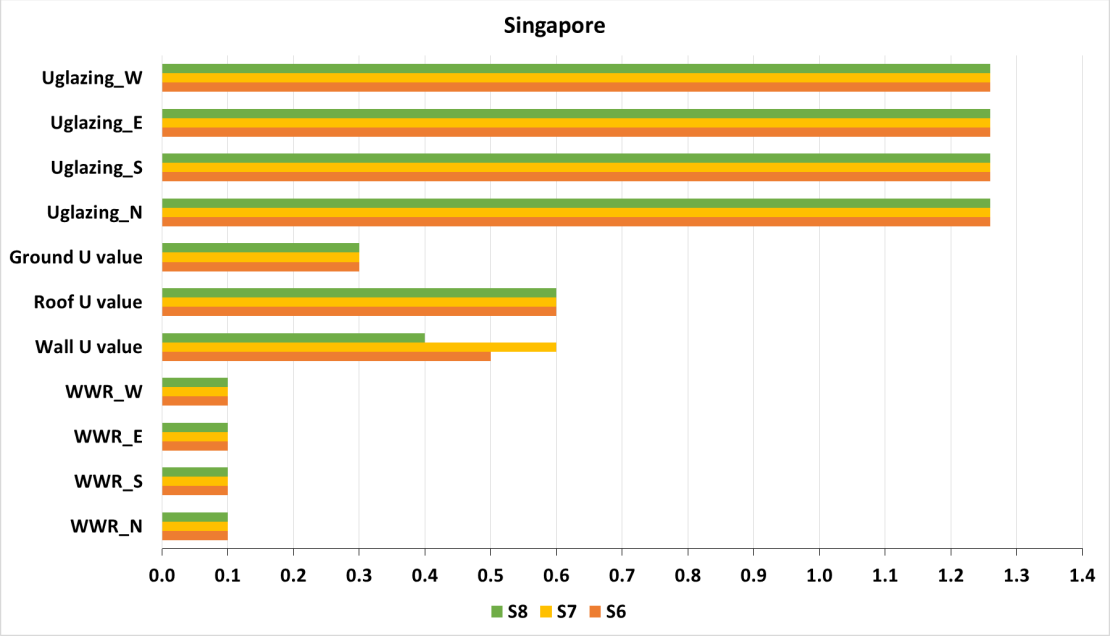

Figure 16 Frequent solutions after ELECTRE III application for Singapore-Category 2

As it could be seen, the sensitivity analysis approves the results since the ranking of the Pareto optimal points does not change significantly in most cities. For example, in Chita, Nancy, Sapporo, Barentsburg and New Delhi the obtained ranking of the optimal point is the same no matter the DM preferences. The sensitivity analysis phase steps are summarized in Figure 17.

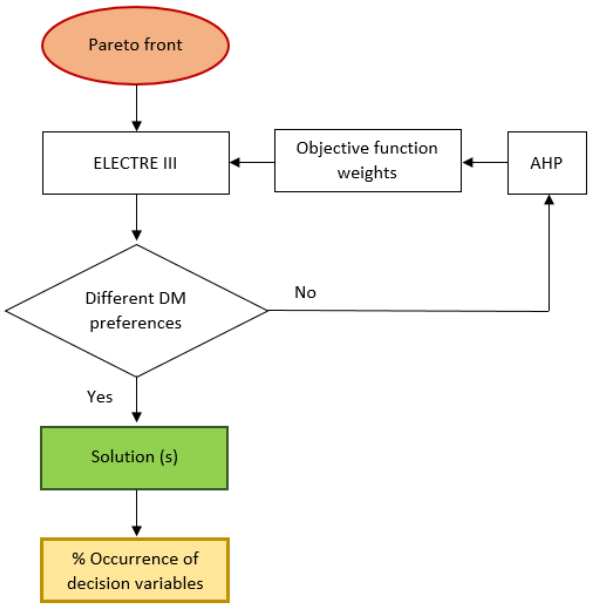

Figure 17 Sensitivity analysis phase steps

Afterward, the percentage of times at which each decision variable has occurred in the final solutions is derived for each category. The decision variables with the highest percentage of occurrence are selected to be the optimal solutions representative for each category (Table 13). This choice is justified to simplify the finding of only one recommended ultimate solution. Next, the decision variables of Table 13 are implemented in the model for different cities and their impact on each objective function, relative to the base case, is examined (Table 14).

Table 13 Optimal decision variables with the highest percentage of occurrence

Category	WWR (%)				Thermal transmittance (W/m².K)			Ug (W/m².K)			
	North	South	East	West	Wall	Roof	Ground	North	South	East	West
1	0.10	0.10	0.10	0.10	0.20	0.20	0.20	1.26	1.26	1.26	1.26
2	0.10	0.10	0.10	0.10	0.60	0.60	0.50	1.26	1.26	1.26	1.26
3	0.10	0.10	0.10	0.10	0.20	0.20	0.30	0.86	0.86	1.26	1.26

Table 14 Summary of building energy and LCC savings relative to the base case

Region	Qcool (kWh/y.m²)		Qheat (kWh/y.m²)		LCC (1000$)	
	Optimal case	% savings	Optimal case	% savings	Optimal case	% savings
Category 1						
Kotelny Island	0.00	-	221.61	65%	86.25	37%
Barentsburg	0.00	-	141.54	67%	139.67	52%
Tromso	0.01	98%	76.11	71%	105.20	48%
Chita	2.01	39%	118.83	65%	73.22	27%
Nancy	4.05	20%	32.06	74%	88.45	33%
Dras	2.70	51%	80.93	66%	62.81	27%
Sapporo	7.30	-3%	43.70	69%	89.61	14%
Khabarovsk	6.63	11%	90.82	65%	70.84	22%
Montreal	7.91	20%	58.44	67%	52.30	8%
Category 2						
Dakar	68.61	54%	0.00	-	93.88	36%
Indore	74.65	49%	0.00	-	48.48	33%
New Delhi	87.51	45%	2.76	-92%	50.61	32%
Singapore	89.87	46%	0.00	-	81.52	32%
Abu Dhabi	99.60	48%	0.00	-	32.25	34%

Caracas	81.22	47%	0.00	-	31.62	34%
Douala	87.15	45%	0.00	-	77.04	32%
Category 3						
Milan	13.77	23%	24.91	73%	111.96	28%
Beijing	20.45	5%	32.59	66%	52.89	13%
Sacramento	23.72	44%	5.33	81%	93.03	9%
Ankara	16.92	29%	22.89	75%	73.76	20%
Cedars	14.82	44%	18.73	72%	92.70	16%
Hakkari	18.65	37%	36.71	67%	78.14	22%
Baku	24.69	29%	15.35	73%	56.53	16%
Esfahan	37.48	33%	9.87	73%	43.09	1%
Kunming	13.21	36%	3.22	87%	47.14	3%

5.2. Discussion of optimal solutions

It is commonly agreed that the passive design requirements vary with the climates. In severe cold climates where the heating is the main load, category 1, the temperature inside the building is typically greater than the outside. Consequently, heat is dissipated through the building envelope. Thus, it is effective to restrict the heat flow through a high level of insulation. Hence, it makes sense the selection of low thermal transmittance 0.2 W/m^2.K for building walls, roof, and ground and 1.26 W/m^2.K for windows. On the other hand, the selection of the correct WWR is essential. The WWR is limited to 10% at each façade, because even the highest performing glazing, triple glazing with Ug = 0.86 W/m^2.K for example, has a much higher thermal transmittance than a typical wall (U < 0.6 W/m2.k). It is worth to mention that the optimal Southern WWR in cold climates (Category 1) would be larger if the aim was only to decrease the heating load (single objective optimization), Table 15. The Southern WWR in Chita and Sapporo would reach 70% and 80% respectively in order to increase heat gains during daytimes.

Table 15 Optimal WWR for single objective optimization (Minimize heating load) in cold climates (Category 1)

Region	**WWR (%)**			
(Category 1)	**North**	**South**	**East**	**West**
Nancy	0.2	0.6	0.2	0.1
Sapporo	0.2	0.8	0.1	0.5
Montreal	0.1	0.5	0.1	0.2
Tromso	0.1	0.5	0.1	0.1
Kotlney Island	0.1	0.1	0.1	0.1
Chita	0.1	0.7	0.1	0.1

Dras	0.2	0.6	0.5	0.2
Barentsburg	0.1	0.3	0.1	0.1

In hot climates, category 2, it is not necessary to resort to high levels of insulation in walls, roof, and ground. As shown in Table 13, the acceptable thermal transmittances of walls, roof and ground are 0.6 W/m^2.K, 0.6 W/m^2.K, and 0.5 W/m^2.K respectively. This is because the insulated envelope restrains the dissipation of the internal heat gains to the exterior ambient at off-peak temperatures. Thus, the heat will be stored in the building which contributes to an increase in the cooling loads. So, the thermal insulation of building envelope in hot climates has a restrictive role. On the other hand, a low WWR and low emissivity double glazing (Thermal transmittance of glazing = 1.26 W/m^2.K) are required to ensure the limitation of heat transmitted through windows from the outside.

For category 3, where both cooling and heating loads coexist, it could be noticed that the walls and roof must be well insulated (Thermal transmittance = 0.2 W/m^2.K). Inversely, the thermal transmittance of ground (0.3 W/m^2.K) should not be decreased to the maximum with the aim to allow the heat to escape through the ground in summer. The low WWR (10%), and well-insulated glazing are optimal to keep as low as possible the heat loss through windows to/from the external environment.

It should be mentioned here that the indoor natural lighting, which is directly affected by the WWR, is not addressed in this study. Even a low value of WWR (10%) is appreciated to enhance the building energy performance, but in practice, it must be accurately determined according to the indoor lighting requirements.

The results obtained in Table 14 reveal that the objective functions were significantly improved after optimization. It is obvious that the implementation of the optimal combination of envelope passive design parameters leads to considerable energy and LCC savings.

In cold climates, the reduction of annual heating load ranges from 65% in Kotelny Island and Khabarovsk up to 74% in Nancy compared to the base case building model. Likewise, the annual cooling load savings for hot climates vary from 45% in New Delhi and Douala up to 54% in Dakar. For category 3, the heating load reaches a value less than 15 kWh/y.m^2 in Milan, Cedars and Kunming, while the cooling load becomes less than 10 kWh/y.m^2 in Sacramento, Esfahan, and Kunming. Consequently, the reduction of thermal loads leads to a clear decrease in LCC in all cities.

The National Renewable Energy Laboratory (NREL) [120] developed a benchmark for low energy building's envelope. When comparing the obtained optimal decision variables in this study with the benchmark recommendation, it can be noticed that the results are within the acceptable range for most passive parameters; see Table 16. Noting that the slight difference is due to the fact that the LCC is one of the objective functions to be minimized in this study.

Table 16 Comparison of the optimal decision variables with the benchmark recommendation

Category	WWR		Ug (W/m².K)		U (W/m².K)					
					Walls		Roof		Ground	
	Optimal	Benchmark	Optimal	Benchmark	Optimal	Benchmark	Optimal	Benchmark	Optimal	Benchmark
1	10%	15%	1.26	1.98	0.2	0.27-0.31	0.2	0.11	0.2	0.15-0.2
2			1.26	2.1	0.6	0.43	0.6	0.18	0.5	0.43
3			0.86-1.26	1.98	0.2	0.31-0.43	0.2	0.15	0.3	0.2-0.3

Most previous studies on building envelope optimization are limited to keep as low as possible the energy demands without considering the occupants' comfort. Thus, the next paragraph will be concerned with inspecting occupant's adaptive comfort in the optimized building for each city, as well as the integration of adequate passive cooling strategies (blinds and/or natural ventilation) to guarantee occupants' thermal comfort.

6. Thermal comfort evaluation

In this section, a thermal assessment is performed to inspect the impact of optimal passive designs on indoor thermal comfort. It is essential to ensure a comfortable indoor climate regardless of the outdoor climate. In this study, the thermal comfort is investigated alone without being implemented within the optimization problem as a constraint. The intention behind this step is to ensure the comfort of each room separately and to visualize what is happening in each room after implementing successively the optimal designs, then the passive cooling strategies, and finally controlling the AC system. On the other hand, this choice demonstrates the fact that even though the minimal thermal loads and LCC are attained, it doesn't mean that the low energy building is now comfortable for occupants.

6.1. Adaptive comfort model

Buildings' energy consumption is strongly dependent on the benchmarks adopted during the design phase for internal cooling and/or heating set points, ventilation rates, lighting, systems operation and comfort analysis. The European standard EN 15251 [52], adopted in this study, specifies different criteria for thermal comfort as well as indoor air quality according to the indoor level of expectation.

In residential building, for periods during which the cooling system is turned off (or do not exist), the acceptable indoor operative temperature's upper and lower limits, $T_{i\,max}$ and $T_{i\,min}$, are derived as a function of the exponentially weighted running mean of outdoor dry-bulb air temperature (T_{rm}) as follows in eq. 4, eq. 5 and eq. 6 [52]. Where T_{ed-k} is the daily mean external temperature for the k^{th} previous day.

$$T_{i\,max} = 0.33T_{rm} + 18.8 + 3\ ;\ 10^{\circ}\mathrm{C} < T_{rm} < 30^{\circ}\mathrm{C} \qquad \text{eq. 4}$$

$$T_{i\,min} = 0.33T_{rm} + 18.8 - 3;\ 15^{\circ}\mathrm{C} < T_{rm} < 30^{\circ}\mathrm{C} \qquad \text{eq. 5}$$

$$T_{rm} = (1-\alpha)\left(T_{ed-1} + \alpha\, T_{ed-2} + \alpha^2 T_{ed-3}\ldots\right);\ \alpha \text{ is recommended to be 0.8 [52]} \qquad \text{eq. 6}$$

The long-term assessment of the thermal comfort conditions according to EN ISO 7730 is estimated based on the method "Percentage outside the range" [121]. In order to avoid the overheating, i.e. uncomfortable hot feelings, the percentage of occupied hours during which the difference ($T_i - T_{i\,\max}$) is greater than or equal to 1˚K during the period from May to September inclusive shall not surpass 3% in each room [122]. The optimal model's overheating level is tested for all cities of categories 1, 2 and 3 accordingly. Then the percentage of overheating hours of the whole building is computed according to eq. 7.

$$\%\ \text{overheating hours} = \frac{\sum \textit{occupied overheating hours in all rooms}}{\sum \textit{occupied hours in all rooms}} \qquad \text{eq. 7}$$

The overheating percentage is zero in all cities of category 1. Figure 18 illustrates the percentage of overheating hours for categories 2 and 3. It can be noticed that the percentages of overheating hours range from 43% in Dakar (Hot semi-arid climate) up to 81% in Singapore (Tropical

rainforest climate), and from 27% in Milan (Humid subtropical climate) up to 45% in Esfahan (Cold desert climate). Afterward, to lessen the obtained high discomfort values, some passive cooling strategies (blinds, natural ventilation) are integrated into the model to find the appropriate combination that decreases the discomfort level to the minimum.

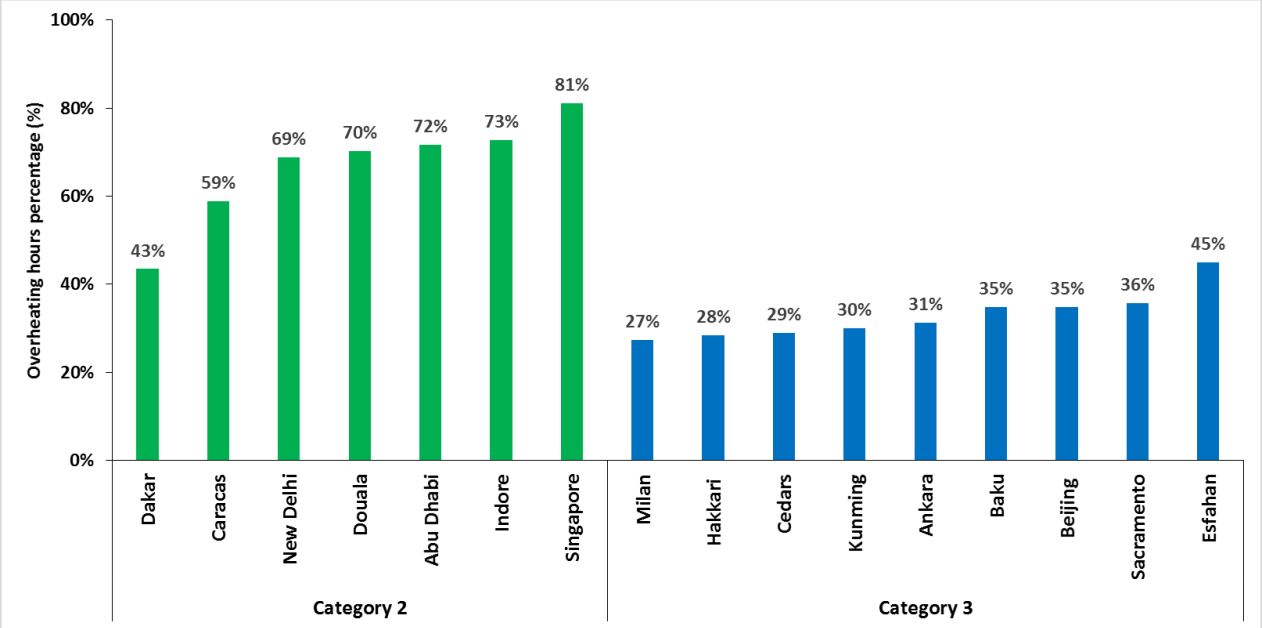

Figure 18 Percentage of overheating hours for categories 2 and 3

6.2. Enhancement of occupants adaptive comfort, cooling load and LCC

In this section, passive cooling strategies including blinds and natural ventilation are investigated to examine their influence on overheating hours, cooling load, and LCC. Other conditions that may influence the control of natural ventilation and blinds, such as glare evaluation, illumination level from the sun, external natural views, and psychology of occupants, are not addressed in this study.

The integrated blinds are external white color roller shutters from ISOTRA [123]. Blinds characteristics according to the standards CSN EN 13363-1+A1 are as follows: reflectivity = 0.7, absorption capacity = 0.3, total solar transmittance factor = 0.047, and reduction coefficient = 0.061. The selection of an external shade is due to its better performance in decreasing the cooling loads than the internal ones [124].

Natural ventilation is an effective passive cooling strategy to reduce cooling demand in buildings. The natural ventilation through windows is due to wind and buoyancy effect. Natural ventilation

performance is measured through the air change rate. Gidds and Phaff [125] derived the air change rate (Air Changer per Hour, ACH) in terms of parameters related to the external environment, window size, and room volume as given by eq. 8.

$$ACH = \frac{1}{2} \times \frac{3600}{V} \times A_W \times \sqrt{0.001\, V_w^2 + 0.0035 H \Delta T + 0.01} \quad \text{eq. 8}$$

Where V is the room's volume (m^3), A_W is the window area (m^2), H is the window height (m).V_W stands for the site mean wind speed (m/s) and ΔT is the mean temperature difference between inside and outside (˚K).

The main challenge associated with natural ventilation design is to find the best flow rate (% of window opening) and the time during which the window must be opened in order to appropriately adjust its control. The obtained minimum sufficient air flow rates of natural ventilation including the control settings are summarized in Table 17.

Table 17 Options of passive cooling design strategies

Strategy	Passive strategies	Control settings
0	No Passive strategies	
1	Blinds during daytime	Category 2: All months Category 3: May-October
2	Ventilation ACH=1, nighttime 9 PM-6 AM	Category 2: Bedrooms, Living, and dining: April-November Kitchen: All months Category 3: Bedrooms, Living, and dining: May-October Kitchen: All months
3	Ventilation ACH=1, all hours	
4	Ventilation ACH=1.5, nighttime 9 PM-6 AM	
5	Ventilation ACH=1.5, all hours	

The presented different cases of natural ventilation are combined with the case of blinds to find the best configuration that ensures the maximum occupants' comfort. Afterward, in case the passive cooling strategies are not able to ensure the requested occupants' adaptive comfort during the occupied periods, the AC is turned ON at 26˚C in the room where the overheating could not be treated. The corresponding percentage of window opening might be controlled using eq. 8. For example, under the weather conditions of Indore region, 1 ACH corresponds to 10% of the window opening in bedrooms and 15% of windows opening in kitchen and living room.

Table 18 summarizes the recognized best passive cooling strategies combination for each city. Moreover, the updated percentage of overheating hours is calculated accordingly and represented in Figure 19.

Table 18 Summary of the optimal passive cooling design strategies for each city

City	Passive Strategies	City	Passive Strategies
Category 2		**Category 3**	
Indore	All rooms: Strategy 1 + Strategy 2	**Baku**	Bedrooms, Living and dining: Strategy 1 Kitchen: Strategy 1+ Strategy 2
Caracas	Bedrooms: Strategy 0 Kitchen: Strategy 1+ Strategy 4 Living and dining: Strategy 4	**Esfahan**	Bedrooms, Living and dining: Strategy 1 Kitchen: Strategy 1+ Strategy 2
New Delhi	All rooms: Strategy 1	**Milan**	Bedrooms, Living and dining: Strategy 1 Kitchen: Strategy 1+ Strategy 2
Singapore	Bedrooms: Strategy 0 Kitchen: Strategy 1 Living and dining: Strategy 1 + Strategy 2	**Sacramento**	Bedrooms, Living and dining: Strategy 1 Kitchen: Strategy 1+ Strategy 4
		Ankara	Bedrooms, Living and dining: Strategy 1 Kitchen: Strategy 1+ Strategy 4
Dakar	Bedrooms: Strategy 0 Kitchen: Strategy 1+ Strategy 3 Living and dining: Strategy 1	**Cedars**	Bedrooms, Living and dining: Strategy 1 Kitchen: Strategy 1+ Strategy 5
Abu Dhabi	All rooms: Strategy 1+ Strategy 4	**Hakkari**	Bedrooms, Living and dining: Strategy 1 Kitchen: Strategy 1+ Strategy 3
Douala	Bedrooms: Strategy 0 Kitchen, Living and dining: Strategy 1+ Strategy 4	**Kunming**	Bedrooms, Living and dining: Strategy 1 Kitchen: Strategy 1+ Strategy 3
		Beijing	Bedrooms, Living and dining: Strategy 1 Kitchen: Strategy 1+ Strategy 2

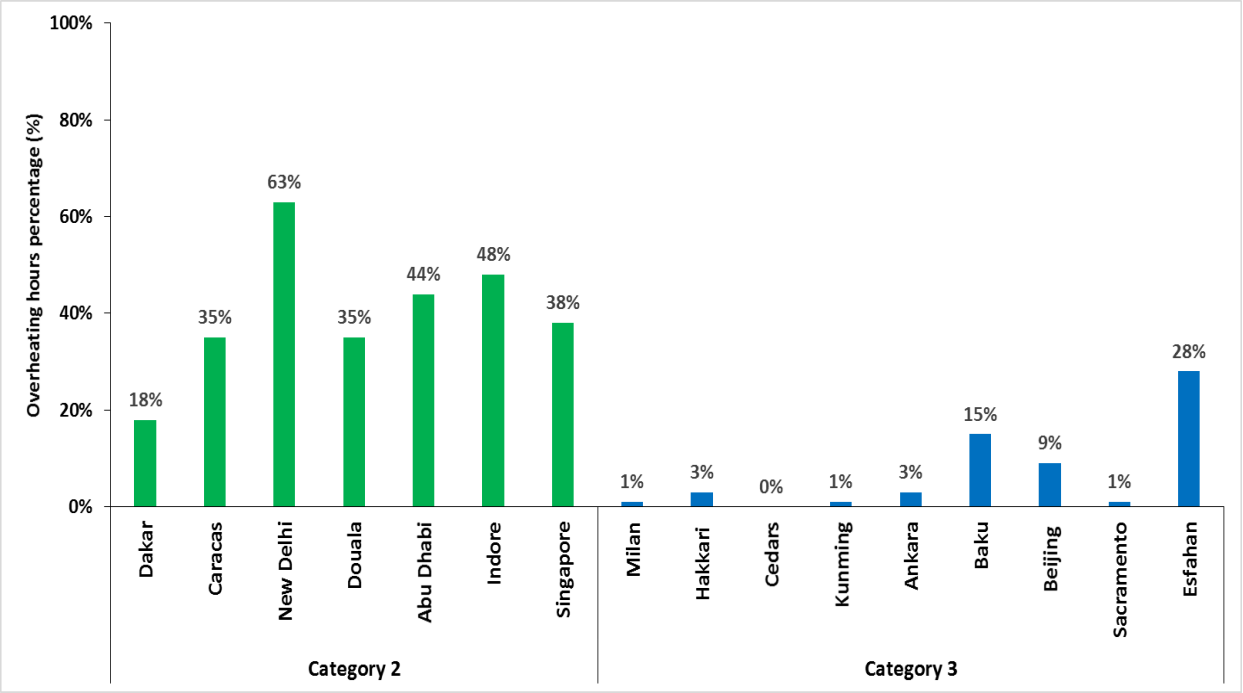

Figure 19 Percentage of overheating hours after implementing the passive cooling strategies

It could be observed that the implementation of passive cooling strategies is practical since the overheating diminution is considerable in almost all cities. The major decrease is found in Singapore, where the introduction of blinds in kitchen and living rooms in addition to the nighttime ventilation (ACH=1) in living room leads to an overheating percentage decrease of 43%. On the other hand, it is clear that the building's average overheating percentage is almost eliminated in many cities of category 3 as shown in Figure 19. The best combinations allow reduction of overheating to become lower than 3% in Milan, Hakkari, Kunming, Ankara, and Sacramento. Besides, 0% overheating in found in Cedars where the AC is no longer crucial. Moreover, the optimal model was sufficient to guarantee the bedrooms' adaptive comfort in Caracas, Singapore, Dakar and Douala climates. The blinds in bedrooms and living room are enough to ensure occupants' comfort in all cities of category 3, see Table 18.

Contrariwise, it is noticed that the natural ventilation in New Delhi doesn't significantly influence the comfort, the natural ventilation plays a drawback role by increasing the cooling needs. Besides, introducing blinds in all rooms of the building in New Delhi is found to be the best solution to slightly decrease the discomfort level from 69% to 63% of overheating hours.

It is important to mention that the increase of the ventilation rate is not a necessary condition to obtain better energy or comfort performances. The nighttime natural ventilation is a fundamental

passive cooling strategy for decreasing discomfort as well as cooling load in zones with high internal heat generation such as kitchens.

It can be observed from Table 19 the months during which the AC is switched ON in each room since the optimal passive cooling strategies failed to completely ensure the occupants' adaptation. It is clear that the AC is turned OFF in bedrooms and living room in all cities excluding Indore, Abu Dhabi, and New Delhi. While in kitchen, where there is a high internal heat generation, the AC must be switched ON for all the year in some regions such as Caracas, Douala, and Singapore. According to results in Table 20, one can notice that the percentages of cooling load savings are considerable, with savings exceeding 50% in all regions except in Indore (13%) and New Delhi (27%).

It is worth mentioning that even though one optimal passive parameters combination is derived for each category (Table 13) when talking about occupants' comfort, each climate has its own scenario and must be treated separately (Table 19 and Table 20).

Table 19 Summary of AC control months in each room

Category	City	AC ON at 26˚C		
		Bedrooms	Living and dining	Kitchen
2	**Indore**	March-September		February-November
	Caracas	OFF	OFF	January-December
	Douala	OFF	OFF	January-December
	Singapore	OFF	OFF	January-December
	Dakar	OFF	OFF	May-November
	Abu Dhabi	April-July		March-September
	New Delhi	May-August	April-September	March-November
3	**Baku**	OFF	OFF	June-August
	Esfahan	OFF	OFF	May-September
	Milan	OFF	OFF	June-August
	Sacramento	OFF	OFF	June-August
	Ankara	OFF	OFF	June-August
	Cedars	OFF	OFF	OFF
	Hakkari	OFF	OFF	July-August
	Kunming	OFF	OFF	April-August
	Beijing	OFF	OFF	June-August

Table 20 Summary of buildings' cooling load, LCC, and savings after introducing passive cooling strategies and taking into account the occupants' adaptive comfort

Category	City	Cooling Load (kWh/y.m^2)	% Savings against optimal case	LCC (1000$)	% Savings against optimal case
2	Indore	48.92	43%	44.40	8%
	Caracas	33.25	59%	28.37	10%
	Douala	31.72	64%	58.03	25%
	Singapore	33.87	62%	61.18	25%
	Dakar	19.98	71%	69.41	26%
	Abu Dhabi	42.42	57%	30.07	7%
	New Delhi	63.77	27%	46.73	8%
3	Baku	6.05	76%	53.79	5%
	Esfahan	11.81	68%	41.35	4%
	Milan	2.74	80%	105.47	6%
	Sacramento	3.59	85%	81.16	13%
	Ankara	4.51	73%	69.58	6%
	Cedars	0.00	100%	84.13	9%
	Hakkari	3.61	81%	73.56	6%
	Kunming	3.15	76%	45.69	3%
	Beijing	5.89	71%	51.00	4%

7. Conclusion

The high potential of buildings towards energy efficiency has drawn special attention to the passive design parameters and passive strategies. In the present paper, a multi-objective decision making optimization is performed on a residential building model under twenty-five different climates of Köppen-Geiger classification. Climates are classified into three categories according to the dominant load (heating, cooling, or both) with the aim to recommend one optimal solution for each category. The simulated building's cooling and heating loads are validated with the experimental results of the NIST residential test facility in Gaithersburg, USA. The implemented methodology is composed of four steps: building energy simulation, optimization, MCDM, and sensitivity study to test the robustness of the obtained optimal result, in addition, passive strategies integration to ensure the occupants' adaptive comfort.

The desired envelope optimal solution is that which minimizes at the same time the building's cooling and/or heating and LCC. A wide range of passive design parameters is investigated including wall and roof insulation levels, windows glazing type and WWR at all facades. The obtained optimal passive parameters are validated with the NREL benchmark for low energy

building's envelope. Besides, to ensure adaptive thermal comfort by decreasing overheating hours, both external shading devices and natural ventilation are examined.

This study has shown that, in severely cold climates, it is efficient to restrict the heat flow through a high level of insulation. Hence the selection of low thermal transmittance of 0.2 W/m^2.K for building walls, roof, and ground and 1.26 W/m^2.K for windows. However, in hot climates, the thermal insulation of building envelope has a restrictive role. It is not needed to use high levels of insulation in the walls, roof, and ground. The appropriate thermal transmittances of walls, roof and ground are 0.6 W/m^2.K, 0.6 W/m^2.K, and 0.5 W/m^2.K respectively. In mixed climates, it is noticed that walls and roof must be well insulated (Thermal transmittance = 0.2 W/m^2.K), whereas the thermal transmittance of ground (0.3 W/m^2.K) should not be decreased to the minimum with the aim to allow the heat evacuation through the ground in summer. Even a low value of WWR (10%) is valuable to enhance the building energy performance, but in practice, it must be accurately determined according to the indoor lighting requirements. The optimal Southern WWR in cold climates would be larger if the aim was only to decrease the heating load (single objective optimization). The Southern WWR in Chita and Sapporo would reach 70% and 80% respectively in order to increase heat gains during daytimes.

The implementation of the optimal combination of envelope passive design parameters leads to considerable energy and LCC savings. The reduction of annual heating loads, cooling loads and LCC reached up to 87% in Kunming, 54% in Dakar and 52% in Barentsburg respectively compared to the base case model.

Moreover, the integrated passive cooling strategies, blinds, and natural ventilation, have demonstrated their competency since they lead to significate cooling load savings that exceeded 50% in almost all regions against the optimal design model. Furthermore, it is clear that the building's average overheating percentage is almost eliminated depending on the category, it becomes lower than 3% in Milan, Hakkari, Kunming, Ankara, and Sacramento, while 0% overheating in found in Cedars where the AC is no longer crucial. Moreover, the optimal model is sufficient to guarantee the bedrooms' adaptive comfort in Caracas, Singapore, Dakar, and Douala climates. Blinds in bedrooms and living room are enough to ensure occupants' comfort in mixed climates. The nighttime natural ventilation with ACH =1-1.5 is a fundamental passive cooling strategy for decreasing discomfort as well as cooling load in kitchens.

An exhaustive study focusing on the influence of uncertainty quantification of the optimal passive design for cooling, heating loads and life cycle cost in each climate will be carried out in the future.

Acknowledgment

The authors would like to acknowledge the Lebanese University, the University of Nice Sophia Antipolis, in addition to the association of specialization and scientific orientation for their support.

References

[1] IEA. International Energy Agency Statistics. 2017. http://www.iea.org (accessed January 15, 2018).

[2] IEA. Transition to sustainable buildings: strategies and opportunities to 2050. IEA Publication; 2013.

[3] Wang L, Gwilliam J, Jones P. Case study of zero energy house design in UK. Energy Build 2009;41:1215–22.

[4] Fong KF, Lee CK. Towards net zero energy design for low-rise residential buildings in subtropical Hong Kong. Appl Energy 2012;93:686–94.

[5] Ibarra LMC, Feldheim V, Dumont E, Pierret S, Deramaix D. Building energy and light simulations for the design of passive apartment buildings in belgium, London, England: 2014.

[6] Bambrook SM, Sproul AB, Jacob D. Design optimisation for a low energy home in Sydney. Energy Build 2011;43:1702–11.

[7] Delgarm N, Sajadi B, Kowsary F, Delgarm S. Multi-objective optimization of the building energy performance: A simulation-based approach by means of particle swarm optimization (PSO). Appl Energy 2016;170:293–303. doi:10.1016/j.apenergy.2016.02.141.

[8] Hassoun A, Dincer I. Development of power system designs for a net zero energy house. Energy Build 2014;73:120–9.

[9] Carlucci S, Cattarin G, Causone F, Pagliano L. Multi-objective optimization of a nearly zero-energy building based on thermal and visual discomfort minimization using a non-dominated sorting genetic algorithm (NSGA-II). Energy Build 2015;104:378–94. doi:10.1016/j.enbuild.2015.06.064.

[10] Zhang L, Zhang L, Wang Y. Shape optimization of free-form buildings based on solar radiation gain and space efficiency using a multi-objective genetic algorithm in the severe cold zones of China. Sol Energy 2016;132:38–50. doi:10.1016/j.solener.2016.02.053.

[11] Azari R, Garshasbi S, Amini P, Rashed-Ali H, Mohammadi Y. Multi-objective optimization of building envelope design for life cycle environmental performance. Energy Build 2016;126:524–34. doi:10.1016/j.enbuild.2016.05.054.

[12] Yang M-D, Lin M-D, Lin Y-H, Tsai K-T. Multiobjective optimization design of green building envelope material using a non-dominated sorting genetic algorithm. Appl Therm Eng 2016. doi:10.1016/j.applthermaleng.2016.01.015.

[13] Kaziolas DN, Bekas GK, Zygomalas I, Stavroulakis GE. Life Cycle Analysis and Optimization of a Timber Building. Energy Procedia 2015;83:41–9. doi:10.1016/j.egypro.2015.12.194.

[14] Hani A, Koiv T-A. Optimization of Office Building Façades in a Warm Summer Continental Climate. Smart Grid Renew Energy 2012;3:222–30. doi:10.4236/sgre.2012.33031.

[15] Asadi E, da Silva MG, Antunes CH, Dias L. A multi-objective optimization model for building retrofit strategies using TRNSYS simulations, GenOpt and MATLAB. Build Environ 2012;56:370–8. doi:10.1016/j.buildenv.2012.04.005.

[16] Bichiou Y, Krarti M. Optimization of envelope and HVAC systems selection for residential buildings. Energy Build 2011;43:3373–82. doi:10.1016/j.enbuild.2011.08.031.

[17] Tuhus-Dubrow D, Krarti M. Genetic-algorithm based approach to optimize building envelope design for residential buildings. Build Environ 2010;45:1574–81. doi:10.1016/j.buildenv.2010.01.005.

[18] Krarti M, Ihm P. Evaluation of net-zero energy residential buildings in the MENA region. Sustain Cities Soc 2016;22:116–25. doi:10.1016/j.scs.2016.02.007.

[19] Cho J, Kim J, Lee S, Koo J. A bi-directional systematic design approach to energy optimization for energy-efficient buildings. Energy Build 2016;120:135–44. doi:10.1016/j.enbuild.2016.03.066.

[20] Sun Y, Huang P, Huang G. A multi-criteria system design optimization for net zero energy buildings under uncertainties. Energy Build 2015;97:196–204. doi:10.1016/j.enbuild.2015.04.008.
[21] Carlucci S, Pagliano L. An optimization procedure based on thermal discomfort minimization to support the design of comfortable net zero energy buildings. Proc. 13th Conf. Int. Build. Perform. Simul. Assoc. Chambery Fr., vol. 2628, 2013, p. 36903697.
[22] Delgarm N, Sajadi B, Delgarm S, Kowsary F. A novel approach for the simulation-based optimization of the buildings energy consumption using NSGA-II: Case study in Iran. Energy Build 2016. doi:10.1016/j.enbuild.2016.05.052.
[23] Ferrara M, Fabrizio E, Virgone J, Filippi M. A simulation-based optimization method for cost-optimal analysis of nearly Zero Energy Buildings. Energy Build 2014;84:442–57. doi:10.1016/j.enbuild.2014.08.031.
[24] Liu S, Meng X, Tam C. Building information modeling based building design optimization for sustainability. Energy Build 2015;105:139–53. doi:10.1016/j.enbuild.2015.06.037.
[25] Almeida M, Bencresciuto A, Ferreira M, Rodrigues A. Cost-effective Energy and Carbon Emission Optimization in Building Renovation – A Case-Study in a Low Income Neighbourhood. Energy Procedia 2015;78:2403–8. doi:10.1016/j.egypro.2015.11.203.
[26] Karaguzel OT, Zhang R, Lam KP. Coupling of whole-building energy simulation and multi-dimensional numerical optimization for minimizing the life cycle costs of office buildings. Build Simul 2014;7:111–21. doi:10.1007/s12273-013-0128-5.
[27] Lu Y, Wang S, Shan K. Design optimization and optimal control of grid-connected and standalone nearly/net zero energy buildings. Appl Energy 2015;155:463–77. doi:10.1016/j.apenergy.2015.06.007.
[28] Lin Y-H, Tsai K-T, Lin M-D, Yang M-D. Design optimization of office building envelope configurations for energy conservation. Appl Energy 2016;171:336–46. doi:10.1016/j.apenergy.2016.03.018.
[29] Xu W, Chong A, Karaguzel OT, Lam KP. Improving evolutionary algorithm performance for integer type multi-objective building system design optimization. Energy Build 2016;127:714–29. doi:10.1016/j.enbuild.2016.06.043.
[30] Harmathy N, Magyar Z, Folić R. Multi-criterion optimization of building envelope in the function of indoor illumination quality towards overall energy performance improvement. Energy 2016;114:302–17. doi:10.1016/j.energy.2016.07.162.
[31] Baglivo C, Congedo P, Fazio A, Laforgia D. Multi-objective optimization analysis for high efficiency external walls of zero energy buildings (ZEB) in the Mediterranean climate. Energy Build 2014;84:483–92.
[32] Asadi E, Silva MG da, Antunes CH, Dias L, Glicksman L. Multi-objective optimization for building retrofit: A model using genetic algorithm and artificial neural network and an application. Energy Build 2014;81:444–56. doi:10.1016/j.enbuild.2014.06.009.
[33] Magnier L, Haghighat F. Multiobjective optimization of building design using TRNSYS simulations, genetic algorithm, and Artificial Neural Network. Build Environ 2010;45:739–46. doi:10.1016/j.buildenv.2009.08.016.
[34] Delgarm N, Sajadi B, Delgarm S. Multi-objective optimization of building energy performance and indoor thermal comfort: A new method using artificial bee colony (ABC). Energy Build 2016;131:42–53. doi:10.1016/j.enbuild.2016.09.003.
[35] Ascione F, Bianco N, De Stasio C, Mauro GM, Vanoli GP. Multi-stage and multi-objective optimization for energy retrofitting a developed hospital reference building: A new approach to assess cost-optimality. Appl Energy 2016;174:37–68. doi:10.1016/j.apenergy.2016.04.078.

[36] Carlucci S, Pagliano L, Zangheri P. Optimization by Discomfort Minimization for Designing a Comfortable Net Zero Energy Building in the Mediterranean Climate. Adv Mater Res 2013;689:44–8.
[37] Ascione F, De Masi RF, de Rossi F, Ruggiero S, Vanoli GP. Optimization of building envelope design for nZEBs in Mediterranean climate: Performance analysis of residential case study. Appl Energy 2016;183:938–57. doi:10.1016/j.apenergy.2016.09.027.
[38] Bojic M, Patou-Parvedy A, Boyer H. Optimization of thermal comfort in building through envelop design. International Conference on Efficiency, Cost, Optimization, Simulation and Environmental Impact of Energy Systems,ECOS 2012, Perigia, Italy, 2012, p. 1–10.
[39] Hasan A, Palonen M, Hamdy M. Simulation-Based Optimization for Energy and Buildings. In: Sayigh A, editor. Renew. Energy Serv. Mank. Vol I, Cham: Springer International Publishing; 2015, p. 503–13.
[40] Mytafides CK, Dimoudia A, Zorasa S. Transformation of a university building into a zero energy building in Mediterranean climate. Energy Build 2017. doi:10.1016/j.enbuild.2017.07.083.
[41] Hopfe CJ, Hensen JLM. Uncertainty analysis in building performance simulation for design support. Energy Build 2011;43:2798–805. doi:10.1016/j.enbuild.2011.06.034.
[42] Gou S, Nik VM, Scartezzini J-L, Zhao Q, Li Z. Passive design optimization of newly-built residential buildings in Shanghai for improving indoor thermal comfort while reducing building energy demand. Energy Build 2017. doi:10.1016/j.enbuild.2017.09.095.
[43] Peleš S, Ahuja S, Narayanan S. Uncertainty quantification in energy efficient building performance simulations. Proc. 2nd Int. High Perform. Build. Conf., 2012.
[44] Harkouss F, Fardoun F, Biwole PH. Multi-Objective Decision Making Optimization of a Residential Net Zero Energy Building in Cold Climate, Lebanon: International Conference on Sensors, Networks, Smart and Emerging Technologies (SENSET). IEEE; 2017.
[45] Harkouss F, Fardoun F, Biwole PH. Multi-objective optimization methodology for net zero energy buildings. J Build Eng 2018;16:57–71. doi:10.1016/j.jobe.2017.12.003.
[46] Harkouss F, Fardoun F, Biwole PH. Optimization of design parameters of a net zero energy home, Lebanon: 3rd International Conference on Renewable Energies for Developing Countries (REDEC). IEEE; 2016.
[47] Deb K, Pratap A, Agarwal S. A fast and elitist multiobjective genetic algorithm: NSGA-II. IEEE Transactions on Evolutionary Computation 2002;6:182–97.
[48] Bai Q. Analysis of Particle Swarm Optimization Algorithm. Comput Inf Sci 2010;3.
[49] Pirim H, Bayraktar E, Eksioglu B. Tabu Search: A Comparative Study. 2008.
[50] Krishnapriya S, Khaleelur Rahiman PF. A survey on Non-dominated sorting genetic algorithm II and its applications. Int J Res Comput Appl Robot 2016;4:7–11.
[51] YAN G, Li C. An Effective Refinement Artificial Bee Colony Optimization Algorithm Based On Chaotic Search and Application for PID Control Tuning. J Comput Inf Syst 2011:3309–16.
[52] European standard NF EN 15251: Indoor environmental input parameters for design and assessment of energy performance of buildings addressing indoor air quality, thermal environment, lighting and acoustics 2007.
[53] Bre F, Fachinotti VD. A computational multi-objective optimization method to improve energy efficiency and thermal comfort in dwellings. Energy Build 2017;154:283–94. doi:10.1016/j.enbuild.2017.08.002.
[54] Ning H, Wang Z, Zhang X, Ji Y. Adaptive thermal comfort in university dormitories in the severe cold area of China. Build Environ 2016;99:161–9. doi:10.1016/j.buildenv.2016.01.003.
[55] de Dear R, Kim J, Parkinson T. Residential adaptive comfort in a humid subtropical climate—Sydney Australia. Energy Build 2018;158:1296–305. doi:10.1016/j.enbuild.2017.11.028.

[56] Ruellan M, Park H, Bennacer R. Residential building energy demand and thermal comfort: Thermal dynamics of electrical appliances and their impact. Energy Build 2016;130:46–54. doi:10.1016/j.enbuild.2016.07.029.
[57] Pomfret L, Hashemi A. Thermal Comfort in Zero Energy Buildings. Energy Procedia 2017;134:825–34. doi:10.1016/j.egypro.2017.09.536.
[58] Thapa S, Bansal AK, Panda GK. Thermal comfort in naturally ventilated office buildings in cold and cloudy climate of Darjeeling, India – An adaptive approach. Energy Build 2018;160:44–60. doi:10.1016/j.enbuild.2017.12.026.
[59] Yang L, Yan H, Lam JC. Thermal comfort and building energy consumption implications – A review. Appl Energy 2014;115:164–73. doi:10.1016/j.apenergy.2013.10.062.
[60] Coley D, Herrera M, Fosas D, Liu C, Vellei M. Probabilistic adaptive thermal comfort for resilient design. Build Environ 2017;123:109–18. doi:10.1016/j.buildenv.2017.06.050.
[61] Attia S, Carlucci S. Impact of different thermal comfort models on zero energy residential buildings in hot climate. Energy Build 2015;102:117–28. doi:10.1016/j.enbuild.2015.05.017.
[62] Zhang Y, Chen Q, Zhang Y, Wang X. Exploring buildings' secrets: The ideal thermophysical properties of a building's wall for energy conservation. Int J Heat Mass Transf 2013;65:265–273.
[63] Zhang Y, Zhang Y, Wang X, Chen Q. Ideal thermal conductivity of a passive building wall: Determination method and understanding. Appl Energy 2013;112:967–974.
[64] Zhang Y, Zhang Y, Shi W, Shang R, Cheng R, Wang X. A new approach, based on the inverse problem and variation method, for solving building energy and environment problems: Preliminary study and illustrative examples. Build Environ 2015;91:204–18.
[65] Zeng R, Wang X, Di H, Jiang F, Zhang Y. New concepts and approach for developing energy efficient buildings: Ideal specific heat for building internal thermal mass. Energy Build 2011;43:1081–1090.
[66] ASHRAE. ASHRAE Fundamentals Handbook (SI) 2001.
[67] European standard prEN 15242: Ventilation for buildings — Calculation methods for the determination of air flow rates in buildings including infiltration 2006.
[68] Green Public Procurement: Indoor Lighting Technical Background Report 2011.
[69] Zimmermann J-P, Evans M, Griggs J, King N. Intertek Report R66141. 2012.
[70] Pettit B, Gates C, Hunter Fanney A, M. Healy W. Design Challenges of the NIST Net Zero Energy Residential Test Facility. National Institute of Standards and Technology U.S. Department of Commerce; 2015.
[71] Fanney AH, Payne V, Ullah T, Ng L, Boyd M, Omar F, et al. Net-zero and beyond! Design and performance of NIST's net-zero energy residential test facility. Energy Build 2015;101:95–109.
[72] Kottek M, Grieser J, Beck C, Rudolf B, Rubel F. World Map of the Köppen-Geiger climate classification updated. Meteorol Z 2006;15:259–63. doi:10.1127/0941-2948/2006/0130.
[73] Meteotest. Meteonorm. Version 6.0 2018. www.meteotest.ch (accessed October 12, 2017).
[74] Krarti M. Energy audit of building systems: an engineering approach. 2nd ed. Boca Raton, FL: CRC Press; 2011.
[75] Milan C, Bojesen C, Nielsen MP. A cost optimization model for 100% renewable residential energy supply systems. Energy 2012;48:118–27.
[76] Spain BJD. Spon's first stage estimating handbook. London: Taylor & Francis; 2006.
[77] Eurostat-statistics explained-Natural gas prices, second half of year, 2014-2016 (EUR per kWh) 2016.
[78] World Energy Resources Natural Gas 2016 n.d.
[79] Energy Supply Pricing for Clients Subject to Price Regulation 2011.
[80] Efficiency E. 2008 INDUSTRIAL TECHNOLOGIES MARKET REPORT 2009.
[81] Energy Market Report-Energy research Estore 2016.

[82] Europe's Energy Portal Fuel, Natural Gas and Electricity Prices From Past to Present 2017. https://www.energy.eu/#domestic (accessed June 18, 2017).
[83] Comparison of Electricity Prices in Major North American Cities 2017. http://www.hydroquebec.com/publications (accessed April 1, 2017).
[84] NAGATA K. Utilities have monopoly on power 2011.
[85] The Japan Times 2017.
[86] Abu Dhabi Distribution Co. 2016. https://www.addc.ae/ar-AE/residential/Pages/RatesAndTariffs2017.aspx (accessed November 15, 2017).
[87] Energy Market Authority of Singapore 2017. https://www.ema.gov.sg/Residential_Electricity_Tariffs.aspx (accessed October 13, 2017).
[88] Electricite de France (EDF) 2017. https://www.edf.fr (accessed March 8, 2017).
[89] Global electricity prices by select countries in 2017 (in U.S. dollars per kilowatt hour) 2017. https://www.statista.com/statistics/263492/electricity-prices-in-selected-countries/ (accessed August 10, 2017).
[90] WHOLESALE GAS PRICE SURVEY 2017 EDITION-A GLOBAL REVIEW OF PRICE FORMATION MECHANISMS-2005 TO 2016 2017.
[91] ANSI/ASHRAE Standard 169, Climatic Data for Building Design Standards. ASHRAE; 2013.
[92] Palonen M, Hamdy M, Hasan A. Mobo a new software for multi-objective building performance optimization. Proc. 13th Int. Conf. IBPSA, 2013, p. 2567–2574.
[93] Nguyen A-T, Reiter S, Rigo P. A review on simulation-based optimization methods applied to building performance analysis. Appl Energy 2014;113:1043–58. doi:10.1016/j.apenergy.2013.08.061.
[94] Evins R. A review of computational optimisation methods applied to sustainable building design. Renew Sustain Energy Rev 2013;22:230–45. doi:10.1016/j.rser.2013.02.004.
[95] Nassif N, Kajl L, Sabourin R. Evolutionary algorithms for multi-objective optimization in HVAC system control strategy. Fuzzy Inf. 2004 Process. NAFIPS 04 IEEE Annu. Meet. Of, Banff, Alberta, Canada, Canada: IEEE; 2004. doi:10.1109/NAFIPS.2004.1336248.
[96] Brownlee AE, Wright JA, Mourshed MM. A multi-objective window optimisation problem. Proc. 13th Annu. Conf. Companion Genet. Evol. Comput., ACM; 2011, p. 89–90.
[97] Palonen M, Hasan A, Siren K. A genetic algorithm for optimization of building envelope and HVAC system parameters, Scotland: Building simulation; 2009.
[98] Lwin K, Qu R, Kendall G. A learning-guided multi-objective evolutionary algorithm for constrained portfolio optimization. Appl Soft Comput 2014;24:757–72. doi:10.1016/j.asoc.2014.08.026.
[99] Machairas V, Tsangrassoulis A, Axarli K. Algorithms for optimization of building design: A review. Renew Sustain Energy Rev 2014;31:101–12. doi:10.1016/j.rser.2013.11.036.
[100] García Kerdan I, Raslan R, Ruyssevelt P. An exergy-based multi-objective optimisation model for energy retrofit strategies in non-domestic buildings. Energy 2016. doi:10.1016/j.energy.2016.06.041.
[101] Hamdy M, Nguyen A-T, Hensen JLM. A performance comparison of multi-objective optimization algorithms for solving nearly-zero-energy-building design problems. Energy Build 2016;121:57–71. doi:10.1016/j.enbuild.2016.03.035.
[102] Yu W, Li B, Jia H, Zhang M, Wang D. Application of multi-objective genetic algorithm to optimize energy efficiency and thermal comfort in building design. Energy Build 2015;88:135–43. doi:10.1016/j.enbuild.2014.11.063.
[103] Yang M-D, Chen Y-P, Lin Y-H, Ho Y-F, Lin J-Y. Multiobjective optimization using nondominated sorting genetic algorithm-II for allocation of energy conservation and renewable energy facilities in a campus. Energy Build 2016;122:120–30. doi:10.1016/j.enbuild.2016.04.027.

[104] Yusoff Y, Ngadiman MS, Zain AM. Overview of NSGA-II for Optimizing Machining Process Parameters. Procedia Eng 2011;15:3978–83. doi:10.1016/j.proeng.2011.08.745.
[105] Kchaou OB, Garbaya A, Kotti M, Pereira P, Fakhfakh M, Helena Fino M. Sensitivity aware NSGA-II based Pareto front generation for the optimal sizing of analog circuits. Integr VLSI J 2016;55:220–6. doi:10.1016/j.vlsi.2016.07.001.
[106] Iniestra JG, Gutierrez JG. Multicriteria decisions on interdependent infrastructure transportation projects using an evolutionary-based framework. Appl Soft Comput 2009;9:512–526. doi:10.1016/j.asoc.2008.07.006.
[107] Fancello G, Carta M, Fadda P. A Decision Support System Based on Electre III for Safety Analysis in a Suburban Road Network. Transp Res Procedia 2014;3:175–84. doi:10.1016/j.trpro.2014.10.103.
[108] Seddiki M, Anouche K, Bennadji A, Boateng P. A multi-criteria group decision-making method for the thermal renovation of masonry buildings: The case of Algeria. Energy Build 2016;129:471–83. doi:10.1016/j.enbuild.2016.08.023.
[109] Żak J, Kruszyński M. Application of AHP and ELECTRE III/IV Methods to Multiple Level, Multiple Criteria Evaluation of Urban Transportation Projects. Transp Res Procedia 2015;10:820–30. doi:10.1016/j.trpro.2015.09.035.
[110] Norese MF. ELECTRE III as a support for participatory decision-making on the localisation of waste-treatment plants. Land Use Policy 2006;23:76–85. doi:10.1016/j.landusepol.2004.08.009.
[111] Marzouk MM. ELECTRE III model for value engineering applications. Autom Constr 2011;20:596–600. doi:10.1016/j.autcon.2010.11.026.
[112] Certa A, Enea M, Lupo T. ELECTRE III to dynamically support the decision maker about the periodic replacements configurations for a multi-component system. Decis Support Syst 2013;55:126–34. doi:10.1016/j.dss.2012.12.044.
[113] Hashemi SS, Hajiagha SHR, Zavadskas EK, Mahdiraji HA. Multicriteria group decision making with ELECTRE III method based on interval-valued intuitionistic fuzzy information. Appl Math Model 2016;40:1554–64. doi:10.1016/j.apm.2015.08.011.
[114] Wu Y, Zhang J, Yuan J, Geng S, Zhang H. Study of decision framework of offshore wind power station site selection based on ELECTRE-III under intuitionistic fuzzy environment: A case of China. Energy Convers Manag 2016;113:66–81. doi:10.1016/j.enconman.2016.01.020.
[115] Lapinskiene V, Martinaitis V. The Framework of an Optimization Model for Building Envelope. Procedia Eng 2013;57:670–7. doi:10.1016/j.proeng.2013.04.085.
[116] Pena RR, Rebollo LP, Gibert K, Valls A. Use and evaluation of ELECTRE III/IV. Universitat Rovira i Virgili; 2007.
[117] Yu X, Zhang S, Liao X, Qi X. ELECTRE methods in prioritized MCDM environment. Inf Sci 2018;424:301–316. doi:10.1016/j.ins.2017.09.061.
[118] Carlucci S, Figueira JR, Greco S, Słowiński R. A robust ranking method extending ELECTREIII to hierarchy of interacting criteria, imprecise weights and stochastic analysis. Omega 2017;73:1–17.
[119] Saaty R. The Analytical Hierarchy Process-What it is and how it is used. Mathl Modelling 1987;9:161–76.
[120] Wilson E, Engebrecht Metzger C, Horowitz S, Hendron R. 2014 Building America House Simulation Protocols. National Renewable Energy Laboratory; 2014.
[121] European standard NF EN ISO 7730: Analytical determinationand interpretation of thermal confort using calculation of the PMV and PPD indicesand local thermal comfort criteria 2006.
[122] Chartered Institution of Building Services Engineers. The limits of thermal comfort avoiding overheating in European buildings ; CIBSE TM52: 2013. London: CIBSE; 2013.
[123] ISOTRA blinds and roller blinds 2018. www.isotra.com (accessed January 14, 2018).
[124] Atzeri A, Cappelletti F, Gasparella A. Internal versus external shading devices performance in office buildings. vol. 45, Energy Procedia; 2014, p. 463 – 472.

[125] Ghiaus C, Allard F, editors. Natural ventilation in the urban environment: assessment and design. Reprint. London: Earthscan; 2007.